Protective T cell immunity in mice following protein-TLR7/8 agonist-conjugate immunization requires aggregation, type I IFN, and multiple DC subsets

Kathrin Kastenmüller,[1] Ulrike Wille-Reece,[1,2] Ross W.B. Lindsay,[1,3] Lauren R. Trager,[1] Patricia A. Darrah,[1] Barbara J. Flynn,[1] Maria R. Becker,[4] Mark C. Udey,[4] Björn E. Clausen,[5] Botond Z. Igyarto,[6] Daniel H. Kaplan,[6] Wolfgang Kastenmüller,[7] Ronald N. Germain,[7,8] and Robert A. Seder[1]

[1]Vaccine Research Center and Cellular Immunology Section, National Institute of Allergy and Infectious Diseases, NIH, Bethesda, Maryland, USA. [2]PATH Malaria Vaccine Initiative, Washington, DC, USA. [3]International AIDS Vaccine Initiative, AIDS Vaccine Design Laboratory, New York, New York, USA. [4]Dermatology Branch, National Cancer Institute, Center for Cancer Research, NIH, Bethesda, Maryland, USA. [5]Department of Immunology, Erasmus University Medical Center, Rotterdam, Netherlands. [6]Department of Dermatology and Center for Immunology, University of Minnesota, Minneapolis, Minnesota, USA. [7]Lymphocyte Biology Section, Laboratory of Immunology, and [8]Program in Systems Immunology and Infectious Disease Modeling, National Institute of Allergy and Infectious Diseases, NIH, Bethesda, Maryland, USA.

The success of a non-live vaccine requires improved formulation and adjuvant selection to generate robust T cell immunity following immunization. Here, using protein linked to a TLR7/8 agonist (conjugate vaccine), we investigated the functional properties of vaccine formulation, the cytokines, and the DC subsets required to induce protective multifunctional T cell immunity in vivo. The conjugate vaccine required aggregation of the protein to elicit potent Th1 $CD4^+$ and $CD8^+$ T cell responses. Remarkably, the conjugate vaccine, through aggregation of the protein and activation of TLR7 in vivo, led to an influx of migratory DCs to the LN and increased antigen uptake by several resident and migratory DC subsets, with the latter effect strongly influenced by vaccine-induced type I IFN. Ex vivo migratory $CD8^-DEC205^+CD103^-CD326^-$ langerin-negative dermal DCs were as potent in cross-presenting antigen to naive $CD8^+$ T cells as $CD11c^+CD8^+$ DCs. Moreover, these cells also influenced Th1 $CD4^+$ T cell priming. In summary, we propose a model in which broad-based T cell–mediated responses upon vaccination can be maximized by codelivery of aggregated protein and TLR7/8 agonist, which together promote optimal antigen acquisition and presentation by multiple DC subsets in the context of critical proinflammatory cytokines.

Introduction

Effective vaccines against a variety of intracellular infections will require Th1 $CD4^+$ T cell responses, $CD8^+$ T cell responses, or both (1). Therefore, development of non-live vaccine platforms that elicit potent T cell immunity is a critical direction in vaccine research, whether for the generation of stand-alone products or for use in combination with viral or live-attenuated vectors to generate strong primary T cell responses and maintain or boost immunity through repeated immunization. Protein-based vaccines are attractive in this context, but optimizing the formulation of such vaccines in terms of physical properties and adjuvant has yet to be achieved with respect to elicitation of potent and protective T cell–mediated immunity rather than humoral immunity (2).

The factors influencing the generation of Th1 $CD4^+$ and $CD8^+$ T cell responses using protein vaccines include the amount, physical form (3) and duration of antigen (4), the cytokine milieu (5, 6), and the type as well as differentiation state of antigen-presenting cells, especially DCs (7, 8). In terms of antigen formulation, it has long been known that particulate antigens are more immunogenic than monomeric proteins for both antibody and T cell immunity (3, 9–15). Moreover, while there are several elegant studies showing how particulate antigens are processed intracellularly for enhanced cross-presentation (10), there is more limited information on how the formulation of the antigen influences the antigen-presenting capacity in vivo in draining LNs (DLNs) after s.c. immunization with a protein vaccine. With regard to the optimal cytokine milieu, adjuvants that induce IL-12 and type I IFN via distinct pattern recognition receptors in DCs (16, 17) and other cells provide the 2 canonical cytokines controlling Th1 differentiation (5) and the cross-presentation of protein antigens to MHC class I–recognizing $CD8^+$ T cells (18, 19). Finally, the extent and efficiency of antigen uptake by the DCs interacting with these T cells is also a critical factor (20). Furthermore, in addition to the established role of certain populations of resident DCs (21), there is now evidence that migratory langerin and dermal DCs also play a critical role in T cell immunity in DLNs from skin (22). Hence, improving the delivery of protein to the specific DC subsets specialized for induction of Th1 immunity or for cross-presentation would provide additional enhancement of the resulting immune response (21).

Taking these factors together, we have directly conjugated protein antigen to a TLR ligand in order to mimic how the immune system may respond to certain infections by having innate stimulation coupled to the antigen, thereby assuring delivery to the same cell (17, 23–25). Indeed, conjugating proteins to TLR2 (Pam3 Cys) (26), TLR5 (flagellin) (27), or TLR9 (CpG ODN) ligands

Authorship note: Kathrin Kastenmüller and Ulrike Wille-Reece contributed equally to this work.

Conflict of interest: The authors have declared that no conflict of interest exists.

Citation for this article: *J Clin Invest.* 2011;121(5):1782–1796. doi:10.1172/JCI45416.

(28–30) enhanced uptake of the conjugate vaccine by DCs and improved antibody and T cell responses compared with protein coadministered with free TLR ligands. Remarkably, uptake of the antigen-CpG conjugate vaccine by DCs was independent of TLR9 activation (31). Hence, the mechanism for the efficiency of the conjugate vaccine for Th1 and cross-presentation vis-à-vis DC processing remains unclear. Further, a potential limitation for the effectiveness of protein-CpG conjugate vaccines for humans is the more limited expression of TLR9 compared with that in mouse DC subsets (32, 33).

For this reason, a protein-conjugate vaccine involving a TLR agonist with the capacity to more broadly target and activate multiple human DC subsets may be critical for using this platform in humans. In this regard, similar to TLR3 and TLR9, TLR7 and TLR8 are expressed intracellularly on ER membranes and endosomes in human plasmacytoid DCs (pDCs) and myeloid DCs (mDCs), respectively (33, 34), and upon activation can induce proinflammatory cytokines and enhance costimulatory function, making ligands for these receptors a potentially potent adjuvant. ssRNA is the natural ligand for TLR7 and TLR8 but is rapidly degraded by RNases in serum, thereby limiting its use as an adjuvant (35–37). Therefore, small synthetic compounds, known as imidazoquinolines, have been developed as alternative adjuvants, operating by activation of TLR7, TLR8, or both (38–43). Stimulation via TLR7 in mice results in production of the proinflammatory cytokine IL-12 by $CD8^-$ DCs (42) and of type I IFN by pDCs (40), providing an optimal cytokine milieu for generating Th1 $CD4^+$ T cells and cross-priming of $CD8^+$ T cells with protein vaccines (19, 44). TLR7 activation also increases expression of costimulatory molecules on DCs and enhances their migration to T cell areas of LNs (42). While originally thought to have minimal activity in mice (41), recent reports show that TLR8 is indeed functional and can regulate TLR7 expression or induce pDC cytokine production after infection with vaccinia virus (43, 45, 46). However, despite these potent effects on innate immunity and DC activation in vitro and in vivo, when not formulated (47) or physically linked to antigen in a vaccine, TLR7/8 agonists show relatively poor adjuvant activity, with respect to inducing cellular immunity in vivo (48, 49). Indeed, prior studies in mice and nonhuman primates showed that HIV Gag protein conjugated to a TLR7/8 agonist induced a much higher frequency of multifunctional Th1 $CD4^+$ T cell and $CD8^+$ T cell responses as compared with the same protein administered with free TLR7/8 agonist.

In this report, we show how the coordinated action of several mechanisms together gives rise to the effectiveness of a protein-TLR7/8 agonist-conjugate vaccine in eliciting strong Th1 $CD4^+$ T cell and $CD8^+$ T cell immunity in vivo. First, protein-TLR7/8 agonist conjugation leads to antigen aggregation, which increases vaccine uptake by all DC subsets (resident and migratory langerin and dermal DCs) in the DLN following s.c. immunization, as compared with nonaggregated protein given with free TLR7/8 agonist. Second, TLR7 activation enhances antigen uptake by DCs in a type I IFN–dependent manner while also promoting migration of DCs to the DLN. In accordance with these findings, both aggregation of the protein and TLR7 activation were required for eliciting optimal cell-mediated immunity. While these data highlight the importance of codelivery of antigen and the innate stimulus to DCs, we also reveal a role for "bystander" production of type I IFN in Th1 development and cross-presentation of antigen to $CD8^+$ T cells. Finally, we show what we believe to be a novel role for $CD8^-DEC205^+CD103^-CD326^-$ langerin-negative dermal DCs and demonstrate, consistent with emerging literature (50), that the activity of multiple distinct DC subsets is important for maximizing Th1 $CD4^+$ T cell and $CD8^+$ T cell responses, and this coordinated activity is promoted by the TLR7/8 agonist linkage to antigen.

Results

Protein-TLR7/8 agonist conjugation leads to increased antigen uptake by $CD11c^+$ DCs. To probe the mechanisms by which the protein-TLR7/8 agonist-conjugate vaccine elicits multifunctional T cell responses, we first examined the uptake of the vaccine by examining the frequency of total $CD11c^+$ DCs that acquired Alexa Fluor 488–labeled (AF488-labeled) OVA protein or AF488-labeled OVA protein conjugated to the TLR7/8 agonist (OVA-conjugate). The total amount of OVA protein administered for all vaccine groups was 20 μg divided into 2 sites. As shown in Figure 1A, the amount of AF488-labeled OVA in $CD11c^+$ DCs following conjugate immunization was substantially higher than that of AF488-labeled OVA protein given with 50 μg free TLR7/8 agonist, which is approximately a 20-fold excess of that contained in the conjugate vaccine. These data highlight the critical contribution of direct conjugation to promoting antigen accumulation in $CD11c^+$ DCs in the DLN following immunization.

Protein-TLR7/8 agonist-conjugate immunization increases DC migration to DLNs. Recently, there have been major advances in delineating the functional specialization of DC subsets migrating from the skin into the DLNs (51–54). We therefore examined how the conjugate vaccine influenced the total number of resident and migratory blood, dermal, and skin-derived DCs in DLNs following s.c. immunization as well as the extent of antigen uptake by these DC subsets. For this analysis a staining panel with the markers CD11c, CD8, B220, DEC205, CD103, CD326, and langerin was used (22, 54, 55) (Figure 1B and Supplemental Figure 1, A and B). Based on the differential expression of these markers, a total of 6 distinct populations of $CD11c^+$ DCs were identified (Figure 1, B and C). These distinct populations are resident $CD11c^+CD8^+$ ($CD8^+$ DCs, subset 1), $CD11c^+B220^+$ (pDCs, subset 2), $CD11c^+CD8^-DEC205^+CD103^-CD326^-$langerin$^-$ (langerin-negative dermal DCs, subset 3A), $CD11c^+CD8^-DEC205^+CD103^-CD326^+$langerin$^+$ (epidermal Langerhans cells [LCs], subset 3B), $CD11c^+CD8^-DEC205^+CD103^+$langerin$^+$ (langerin-positive dermal DCs, subset 4), and $CD11c^+CD8^-DEC205^-CD103^-$ ($CD8^-$ resident and blood-derived DCs, subset 5). To simplify visualization of this complex DC response, the relative proportion of each subset within the total $CD11c^+$ population is depicted in a pie chart (Figure 1C). In PBS-treated mice, $CD11c^+CD8^-DEC205^-$ (subset 5) and langerin-negative dermal DCs (subset 3A) were the largest populations, comprising approximately 30% of total $CD11c^+$ DCs. $CD8^+$ DCs (subset 1) and pDCs (subset 2) comprise approximately 10%–15% of total $CD11c^+$ DCs. Epidermal LCs (subset 3B) and langerin-positive dermal DCs (subset 4) account for approximately 1%–5% and less than 1% of total $CD11c^+$DCs, respectively.

The number and composition of the various DC subsets at 24, 48, and 72 hours after immunization with OVA protein given with or without the free TLR7/8 agonist or immunization with the OVA-conjugate vaccine is shown in Figure 1D. Immunization with OVA plus the free TLR7/8 agonist led to a striking increase in the total number of specific DC subsets in the DLN compared with OVA alone or PBS (data not shown) at all time points after immunization. These changes were mainly accounted for by an increase in the

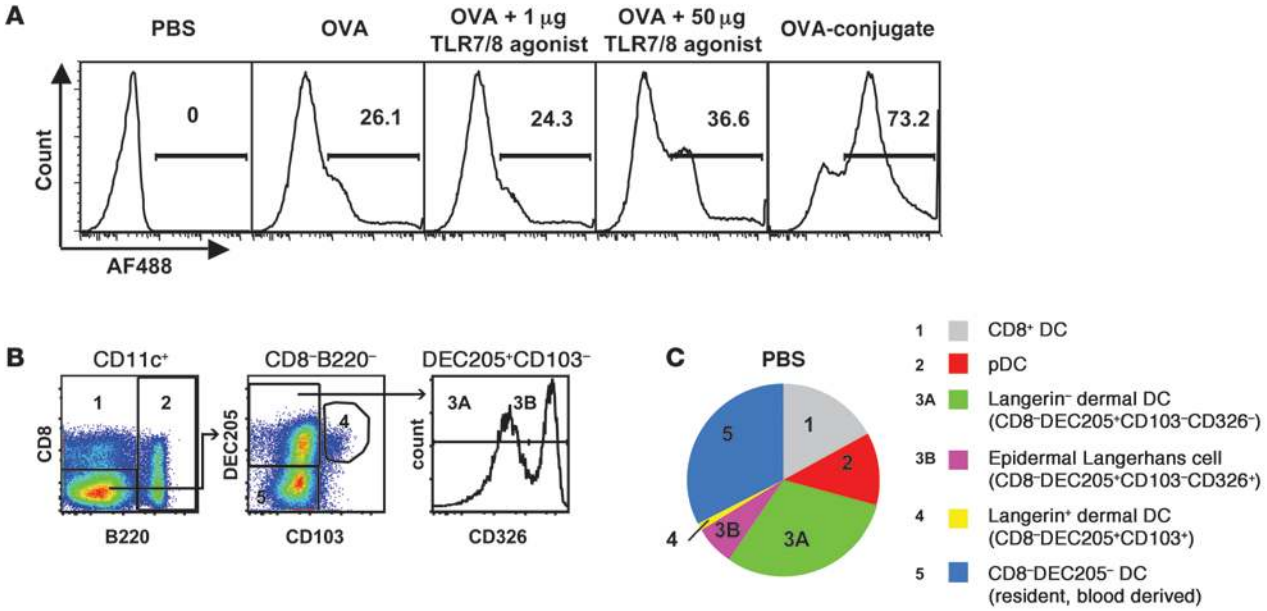
A
PBS
OVA
OVA + 1 μg TLR7/8 agonist
OVA + 50 μg TLR7/8 agonist
OVA-conjugate
0
26.1
24.3
36.6
73.2
Count
AF488
B
CD11c+
CD8−B220−
DEC205+CD103−
CD8
B220
DEC205
CD103
count
CD326
3A
3B
C
PBS
1 CD8+ DC
2 pDC
3A Langerin− dermal DC (CD8−DEC205+CD103−CD326−)
3B Epidermal Langerhans cell (CD8−DEC205+CD103−CD326+)
4 Langerin+ dermal DC (CD8−DEC205+CD103+)
5 CD8−DEC205− DC (resident, blood derived)
D
OVA
OVA + TLR7/8 agonist
OVA-conjugate
Day 1
Day 2
Day 3
Absolute number of CD11c+ DCs
1x10^6
2x10^5
5x10^4
3x10^4
1x10^4
0
DC subset (Pies)
1
2
3A
3B
4
5

Figure 1
OVA vaccines induce distinct changes in the composition of DCs within the DLN. (**A**) Comparison of uptake of AF488-labeled OVA-conjugate (OVA-conj.) versus AF488-labeled OVA, with or without varying amounts of free TLR7/8 agonist 48 hours after immunization in Balb/c mice. Numbers within histograms refer to the percentages of $CD11c^+$ DCs that took up the AF488-labeled OVA protein. Data are representative of 2 independent experiments. (**B**) Following enrichment of $CD11c^+$ DCs from B6 mice (Supplemental Figure 1A), cells were divided into $CD8^+$ DCs (subset 1) and pDCs (subset 2) based on their expression of CD8 and B220. $B220^-CD8^-$ DCs were further categorized as $DEC205^+CD103^+$ (subset 4), $DEC205^+CD103^-$, and $DEC205^-CD103^-$ (subset 5) DC populations based on their expression of CD103 and DEC205, and $DEC205^+CD103^-$ cells were further divided into CD326-positive (Epcam-positive) (subset 3B) and -negative populations (subset 3A). (**C**) Proportions of the different DC subpopulations in LNs of PBS-treated mice. Each DC subset was assigned a number and color based on the gating strategy depicted in **B**. Phenotypic descriptions of the subsets with the matching color codes are shown. The pie chart shows the relative percentage of each DC subset within the total $CD11c^+$ DC population. Data were collected from pooled DLNs of 10 immunized mice. (**D**) Absolute numbers of cells in different DC subpopulations analyzed at different time points after immunization with either OVA, OVA plus free TLR7/8 agonist, or OVA-conjugate (n = 10 mice/group). The distribution of the $CD11c^+$ DC subpopulations in the DLNs is presented as absolute number and the relative proportion (pie charts) of each DC subset at various times after immunization.

population of langerin-negative dermal DCs (subset 3A). Immunization with the OVA-conjugate vaccine led to a further increase in the number of specific DC subsets as compared with that with OVA protein plus the free TLR7/8 agonist. The conjugate vaccine induced an increase in the number of all DC populations, with the exception of the infrequent langerin-positive dermal DCs (subset 4). There was a predominance (~60%) of $CD8^-DEC205^-$ DCs (subset 5) in the expanded population. Overall, these data show that the OVA-conjugate vaccine induces a striking change in the number and composition of $CD11c^+$ DC subsets compared with that with protein plus the free TLR7/8 agonist, with the $CD8^-CD205^-$ DC subpopulation being the most prominent.

Protein-TLR7/8 agonist-conjugate vaccine differentially alters the uptake by DC subpopulations. We next analyzed whether these differences in DLN DC composition after immunization with OVA, OVA plus TLR7/8 agonist, or conjugate vaccine are associated with differential antigen uptake among the distinct DC subsets. As shown in Figure 2A and consistent with Figure 1D, there was an increase in the absolute number of $AF488^+$ DCs in animals immunized with the conjugate vaccine compared with that in animals immunized with OVA plus the free TLR7/8 agonist or OVA alone. While these data are from 24 hours after immunization, similar results were seen at 48 and 72 hours (data not shown). This analysis further showed that on a per cell basis (using MFI as an indicator), OVA was taken up to similar extent by all DC subsets when given with the free TLR7/8 agonist (Figure 2B). However, there was an increase in MFI in pDCs (DC subset 2) and $CD8^-$ resident and blood-derived DCs (DC subset 5) from mice that received the conjugate vaccine compared to mice that received OVA, with or without the free TLR7/8 agonist. It is notable that these DC subsets, with higher MFI, express TLR7 (42, 56). Together, these data show that there is an increase in the fraction of DCs that take up the conjugate vaccine, which we will refer to as uptake, as well as the amount of antigen per cell based on MFI in these 2 DC subsets.

Protein aggregation and type I IFN enhance uptake of the conjugate vaccine by DCs in vivo. To investigate the mechanism(s) by which the OVA-conjugate vaccine mediates its effects on DC antigen uptake, we determined the effect that conjugation had on the form of the protein and whether functional TLR7 activation was required. Using fast protein liquid chromatography, the eluted material revealed the expected monomeric character of the OVA protein, as shown by a single peak (Figure 3A, left). By contrast, conjugation of the OVA protein to the TLR agonist by UV activation resulted in a single peak, which eluted quicker from the column and, therefore, represents aggregated protein (Figure 3A, middle). Last, using the chemical conjugation method, in which the monomeric OVA protein was linked to an active TLR7/8 agonist by chemical conjugation with sulfosuccinimidyl-4- (*N*-maleimidomethyl) cyclohexane-1-carboxylate (SMCC), we detected a heterogeneous mixture of aggregated and monomeric protein conjugate with sizes calculated to be approximately 580 kD and 42 kD, respectively (Figure 3A, right).

To assess separately the influence of protein aggregation and TLR7/8 signaling on DC uptake in vivo, the OVA protein was conjugated by SMCC to an active or a structurally similar but inactive TLR7/8 agonist, and mice were immunized with the purified monomeric or aggregated formulation (Figure 3B). In addition, we assessed uptake with aggregated protein conjugated to the TLR7/8 agonist by UV activation. As shown in Figure 3B, there was enhanced uptake of aggregated versus monomeric OVA conjugated to active (55.6% vs. 17.2%) or inactive (37.9% vs. 8.8%) TLR7/8 agonist or the aggregated UV conjugated protein (53%). Remarkably, there was also an increased frequency of cells with detectable antigen in recipients of the aggregated OVA protein conjugated with the active versus inactive TLR7/8 agonist (55.6% vs. 37.9%), suggesting a role of TLR7 signaling in uptake of the vaccine.

Therefore, we extended the analysis of the potential role of TLR7 signaling on antigen acquisition by examining the frequency of OVA-conjugate vaccine uptake by DCs in WT and TLR7 KO mice (Figure 3C, top). Consistent with the results in Figure 3B, using aggregated protein with an inactive TLR7/8 agonist, the frequency of DCs showing acquisition of the conjugate vaccine in TLR7 KO mice was decreased approximately 2 fold compared with that seen in WT mice (Figure 3C, top). Because type I IFN has been shown to enhance migration and maturation of DCs (42, 57, 58), we hypothesized that TLR7 activation could be mediating its effect(s) on uptake of antigen by DCs in vivo through induction of type I IFN. Indeed, uptake of the OVA-conjugate vaccine in TLR7 KO mice was enhanced when IFN-α was administered together with the vaccine (Figure 3C, top). As a corollary, after conjugate immunization we found a reduction in the frequency of antigen-containing DCs in WT mice treated with anti–IFN-α receptor 1 (anti–IFN-αR-1) prior to immunization or among DCs from IFN-αβ receptor KO mice (Figure 3C, middle). Since TLR7 can also induce IL-12 production by DCs in vivo, which may influence DC migration (59), we determined whether the absence of IL-12 would have an effect on the uptake of the conjugate vaccine. As shown in Figure 3C (bottom), there was no effect on the uptake of the OVA-conjugate vaccine in vivo in IL-12p40 KO mice as compared with WT mice. Last, TLR7 and IFN-αβ receptor KO mice showed approximately 3- to 5-fold reduction in the total number of $CD11c^+$ DCs in the DLN following conjugation immunization (data not shown).

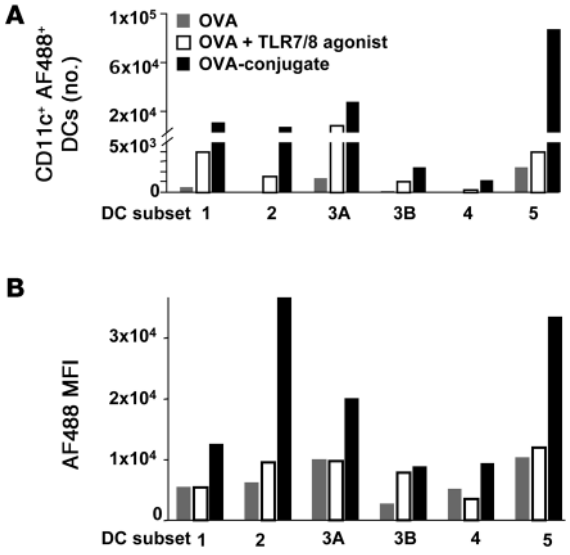

Figure 2
DC subsets differentially take up OVA vaccines. Twenty-four hours after immunization of B6 mice with 20 μg AF488-labeled OVA, AF488-labeled OVA plus free TLR7/8 agonist, or AF488-labeled OVA-conjugate DLNs were harvested, pooled, and enriched for CD11c$^+$ DCs. (**A**) Absolute numbers of the different DC subsets that are AF488 positive. (**B**) MFI of AF488-positive cells within each DC subset. DC subset 1, CD8$^+$ DCs; DC subset 2, pDCs; DC subset 3A, langerin-negative dermal DCs; DC subset 3B, epidermal LCs; DC subset 4, langerin-positive dermal DCs; DC subset 5, CD8$^-$DEC205$^-$ (resident, blood-derived) DCs.

This change in physical state of the antigen also influenced the drainage and uptake of the vaccine in DLNs. As shown in Supplemental Figure 2, monomeric or aggregated OVA conjugated to the active TLR7/8 agonist and labeled with Alexa Fluor 647 (AF647) was present in the cortical region and particularly in the medullary sinus of the DLN at 6 hours after immunization (Supplemental Figure 2A). The signal intensity remaining in the tissue at this time was strikingly higher with aggregated OVA as compared with that with monomeric OVA. Both protein formulations gave fluorescence that overlapped with LYVE-1 staining that marks the lymphatic endothelium lining of the sinuses (Supplemental Figure 2B). Large amounts of aggregated OVA but not monomeric OVA were easily visualized within LN resident DCs 6 hours after immunization (Supplemental Figure 2C). In terms of duration, we could still detect more aggregated OVA in the sinuses of the DLN compared with OVA protein plus the free TLR7/8 agonist at 48 hours after immunization (data not shown). Together, these data show that aggregation has a demonstrable influence on antigen uptake by DCs in vivo, with TLR7/8 activation surprisingly also having an additional effect. In summary, these data establish that aggregation of protein increases uptake of the conjugate vaccine and show that TLR7 activation and type I IFN influence both the number of DCs migrated into the DLN following immunization and the efficacy of uptake of the antigen by CD11c$^+$ DCs.

Aggregated protein conjugated to an active TLR7/8 agonist is required for Th1 CD4$^+$ and CD8$^+$ T cell immunity. Given the critical roles of protein aggregation and TLR7/8 activation for increased accumulation of DCs in the LN and antigen uptake by DCs in vivo, we determined the influence of these factors on the generation of T cell immunity in vivo. As shown in Figure 4A, immunization with aggregated OVA protein conjugated to the active TLR7/8 agonist induced OVA-specific CD4$^+$ and CD8$^+$ cytokine-producing T cells. By contrast, there were low to undetectable T cell responses following immunization with aggregated OVA protein conjugated to the inactive TLR7/8 agonist or monomeric OVA protein conjugated to an active TLR7/8 agonist. These findings for the increase in CD8$^+$ T cell cytokine responses with the short-term in vitro stimulation with OVA peptide are further substantiated by staining with the H-2K^b/OVA$_{257–264}$ tetramer (Figure 4B). Last, coinjection of the free TLR7/8 agonist with aggregated OVA protein conjugated to the inactive TLR7/8 agonist induced low to undetectable T cell responses (data not shown). Together, these data highlight the importance of the combination of protein aggregation and physically linked codelivery with the TLR7/8 agonist for optimizing T cell immunity in vivo (23–25).

To extend the immune analysis, we determined the quality of the T cell responses by delineating the pattern of IL-2, TNF-α, and IFN-γ production capacity at the single-cell level using multiparameter flow cytometry (Supplemental Figure 3) at 10 and 28 days following a single immunization. As shown in Supplemental Figure 3, A and B, the OVA-conjugate vaccine induced potent T cell cytokine responses at the peak of the response (day 10) as well as at 28 days after immunization. Moreover, such responses were multifunctional at both time points (Supplemental Figure 3C). Finally, to establish whether the responses were protective, mice were challenged with recombinant *Listeria monocytogenes* expressing OVA protein. As shown in Figure 5, there was a significant decrease in bacterial load in liver and spleen in the OVA-conjugate immunized mice compared with those immunized with OVA protein with or without free TLR 7/8 agonist ($P < 0.05$). Such responses conferred protection even at 6 weeks after a single immunization with the OVA-conjugate vaccine (Figure 5B). These data demonstrate that the T cell responses are durable and functional in vivo.

TLR7 signaling, type I IFN, and IL-12 are required for maximal T cell immunity in vivo following conjugate immunization. The next series of experiments focused on the requirement of TLR7 activation and production of cytokines, such as type I IFN, for priming T cells in vivo. To examine how these innate pathways influence antigen-specific T cell immunity in vivo, TLR7 KO mice and IFN-αβ receptor KO mice were vaccinated with the OVA-conjugate vaccine and compared with WT mice vaccinated in a similar manner (Figure 6). Because type I IFN was able to restore uptake of the conjugate vaccine by DCs in the absence of TLR7 (Figure 3C), we also assessed how this cytokine influenced T cell activation and priming in vivo independent of TLR7 signaling. As expected, there were no detectable Th1 CD4$^+$ T cell or CD8$^+$ T cell responses in TLR7 KO mice when assessed 7 days after 2 immunizations given 3 weeks apart; however, detectable T cell responses could be induced in TLR7 KO mice immunized with

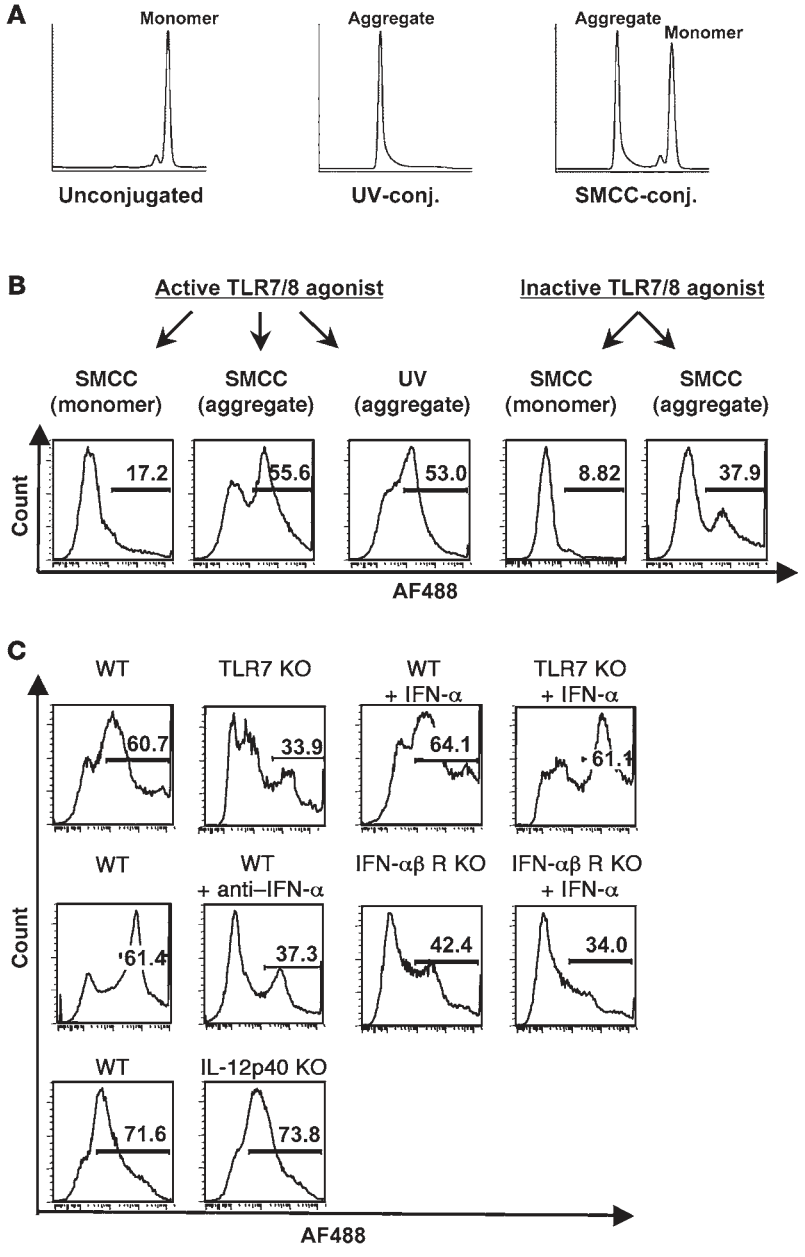

Figure 3
Protein aggregation and IFN-α enhance antigen uptake by CD11c$^+$ DCs in vivo. (**A**) Representative elution profiles of unconjugated OVA and UV-conjugated or chemically conjugated (SMCC-conj.) OVA, using fast protein liquid chromatography. (**B**) BALB/c mice (n = 10) were immunized with the eluted fraction (monomer or aggregate) of the different conjugates linked to AF488, and the percentage of CD11c$^+$ DCs that took up AF488 was analyzed 24 hours later. (**C**) Uptake of OVA-conjugate was assessed in CD11c$^+$ DCs isolated from the DLNs from B6, TLR7 KO, IFN-αβ receptor KO, and IL-12p40 KO mice. In some separate experiments, exogenous IFN-α was injected with the conjugate vaccine or anti–IFNαR-1 was administered intraperitoneally before immunization. (**B** and **C**) Numbers within histograms refer to the percentages of CD11c$^+$ DCs that took up the AF488-labeled OVA protein. Data are representative of at least 2 independent experiments.

the conjugate vaccine and exogenous type I IFN. Thus, some level of T cell immunity can be induced in the absence of TLR7 signaling, but this response is dependent on type I IFN. In agreement with these data, the frequency of cytokine-producing Th1 CD4$^+$ or CD8$^+$ T cell responses was decreased in IFN-αβ receptor KO mice compared with that in WT mice after immunization with the OVA-conjugate. Thus, in the absence of type I IFN signaling, TLR7 activation is sufficient to mediate some level of T cell immunity compared to the T cell responses generated in WT mice. Collectively, these data show that while type I IFN has a critical role in mediating T cell immunity following conjugate immunization, there are other mechanisms by which TLR7 engagement can augment in vivo T cell responses. In this regard, since TLR7 induces production of IL-12p40 and p70 from DCs (42, 56), we next assessed the role of IL-12p40 in determining the magnitude and quality of CD4$^+$ T cell and CD8$^+$ T cell responses.

As shown in Supplemental Figure 4A, the frequencies of total cytokine-producing CD4$^+$ T cells and CD8$^+$ T cells were decreased ~2–3 fold in IL-12p40 KO mice compared with those in WT mice after OVA-conjugate immunization. Moreover, IL-12 had a substantial influence on the quality of Th1 CD4$^+$ and CD8$^+$ T cell responses (Supplemental Figure 4B). Finally, as both IL-12 and type I IFN signaling substantially reduced but did not completely abolish T cell immunity after conjugate immunization, we assessed responses when both of these innate cytokines were inhibited. As shown in Supplemental Figure 5, IFN-αβ receptor KO mice treated with anti–IL-12 had complete inhibition of both CD4 and CD8$^+$ T cell cytokine responses. Thus, both IL-12 and type I IFN induced by TLR7 activation are required for maximal T cell immunity with this conjugate vaccine.

Codelivery of the protein and TLR7/8 agonist is required for IL-12p40 production and CD8 stability in vivo. Synchronous activation of DCs presenting antigen using the TLR ligands LPS or CpG has been shown to enhance CD4$^+$ T cell activation and differentiation of Th1 effector cells (23–25). As TLR7 is expressed in CD11c$^+$CD8$^-$ DCs, which are capable of IL-12 production (42, 56), a critical cytokine for optimal T cell immunity (Supplemental Figure 4A), we examined IL-12p40 production from CD11c$^+$ DCs isolated directly ex vivo after immunizing with different OVA vaccines (Supplemental Figure 4, D and E). Comparing IL-12p40 production after vaccination with the aggregated formulation of OVA linked to the inactive or active TLR7/8 agonist, it was apparent that only linked delivery of protein and active TLR7/8 agonist led to IL-12p40 production. By contrast, even high amounts of the free TLR7/8 agonist were unable to induce intracellular IL-12p40 from CD11c$^+$ DCs in vivo when given with OVA protein (Supplemental Figure 4E). Consistent with previous reports (42, 56), intracellular IL-12p40 was produced by CD8$^-$ but not CD8$^+$ DCs (Supplemental Figure 4E). These data provide important evidence for how conjugation is required for optimizing a critical innate cytokine that is shown to be essential for maximizing T cell immunity in vivo.

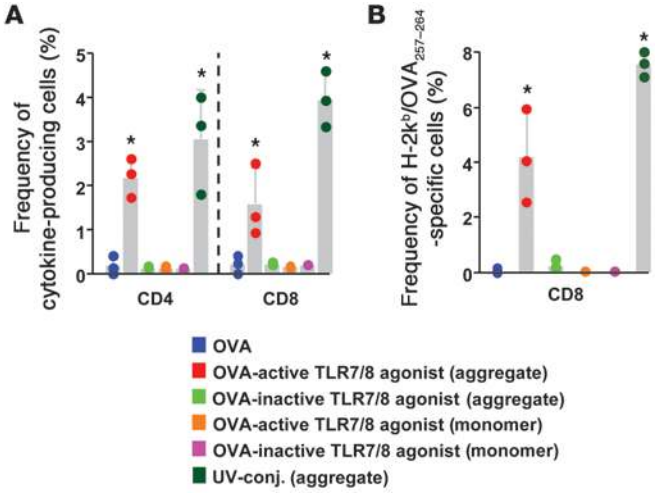

Figure 4
Protein aggregation is required for the induction of OVA-specific T cell responses. B6 mice (n = 3/group) were immunized (s.c.) twice, 3 weeks apart, with 20 μg monomeric or aggregated OVA protein conjugated to an active or inactive TLR7/8 agonist or OVA protein alone. Seven days after the second immunization with the indicated conjugate vaccines, T cells in spleens were analyzed for cytokine production or tetramer binding by flow cytometry. (**A**) Frequency of OVA-specific IFN-γ–, IL-2–, or TNF-α–producing $CD4^+$ or $CD8^+$ T cells. (**B**) Frequency of H-$2K^b$/$OVA_{257–264}$ tetramer–specific $CD8^+$ T cells *$P < 0.05$, comparing aggregated protein conjugated with an active TLR7/8 agonist or the UV-conjugate compared with all other vaccine groups. Each symbol represents an individual mouse.

We next examined the influence of codelivery of antigen and adjuvant on $CD8^+$ T cell immunity. To address this, the fate of adoptively transferred naive antigen-specific OT-I cells was assessed in vivo in DLN and spleen at several time points after immunization with OVA, OVA plus free TLR7/8 agonist, or the conjugate vaccine (Supplemental Figure 6). We found that while vaccination with OVA plus free TLR7/8 agonist did cause some initial proliferation of naive OT-I cells within the first several days after immunization, such cells were not detectable in LN or spleen when assessed 8 days after immunization. By contrast, the conjugate vaccine caused a marked expansion of OT-I cells, and this expanded population persisted over time as compared with OT-I T cells exposed to OVA plus free TLR7/8 agonist. The results again highlight the importance of physically concordant delivery of antigen with a TLR7/8 agonist for maximally effective T cell priming.

$CD8^+$ DCs and migratory $CD8^–CD205^+$ DCs play a critical role in antigen presentation to $CD4^+$ and $CD8^+$ T cells. Because the OVA-conjugate vaccine was taken up by multiple DC subsets in vivo (Figure 2A), in the final series of experiments we examined the role(s) of these distinct cell types in antigen presentation to naive T cells in vitro and priming of T cells in vivo. We first assessed the capacity of various DC subsets to present antigen to naive OVA-specific $CD8^+$ (OT-I) and $CD4^+$ (OT-II) T cells ex vivo. To this end, $CD11^+$ DCs were enriched from pooled DLNs of mice immunized 48 hours previously with

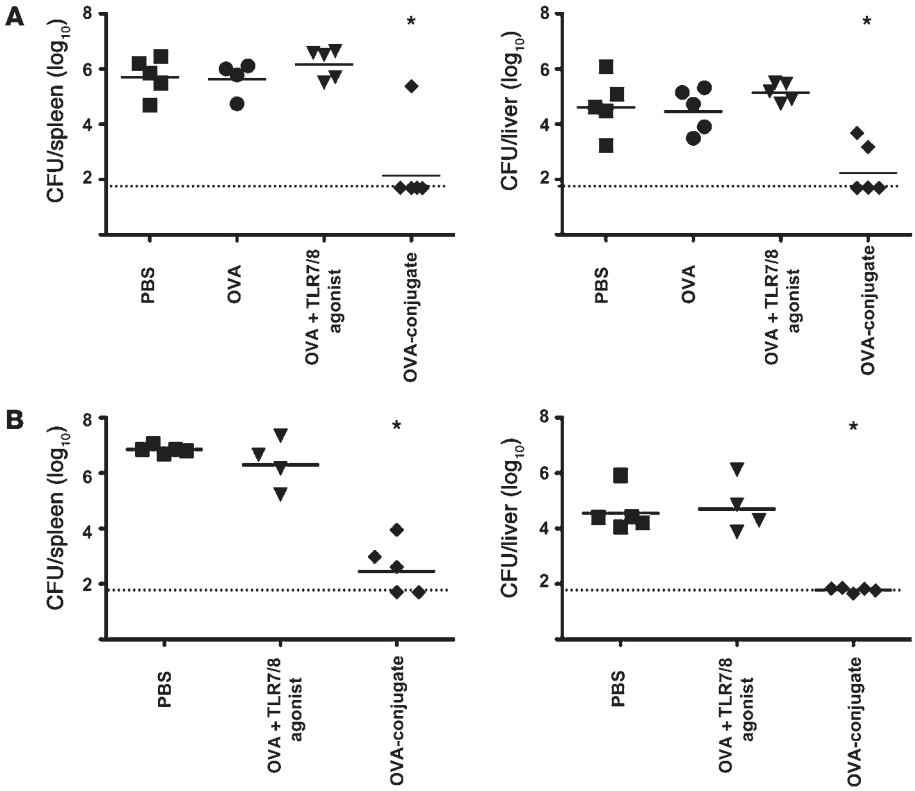

Figure 5
OVA-conjugate vaccine confers protection against *L. monocytogenes* challenge. (**A**) Mice (n = 4-5) were immunized twice, 3 weeks apart, with PBS, 20 μg OVA, OVA plus free TLR7/8 agonist, or the OVA-conjugate vaccine. Fourteen days after the second immunization mice were challenged i.v. with 3×10^4 CFUs of recombinant *L. monocytogenes* OVA. Bacterial loads in spleen and liver were enumerated 3 days after the challenge. (**B**) Mice (n = 4–5) were immunized once with 20 μg OVA plus free TLR7/8 agonist or the OVA-conjugate vaccine or were left untreated. Six weeks after immunization mice were challenged i.v. with 6×10^4 CFUs of recombinant *L. monocytogenes* OVA. Bacterial loads in spleen and liver were enumerated 3 days after the challenge. Solid lines represent the geometrical mean. Dotted lines represents the level of detection. *$P < 0.05$, Mann-Whitney test, comparing OVA-conjugate with all other vaccine groups. Each symbol represents an individual mouse.

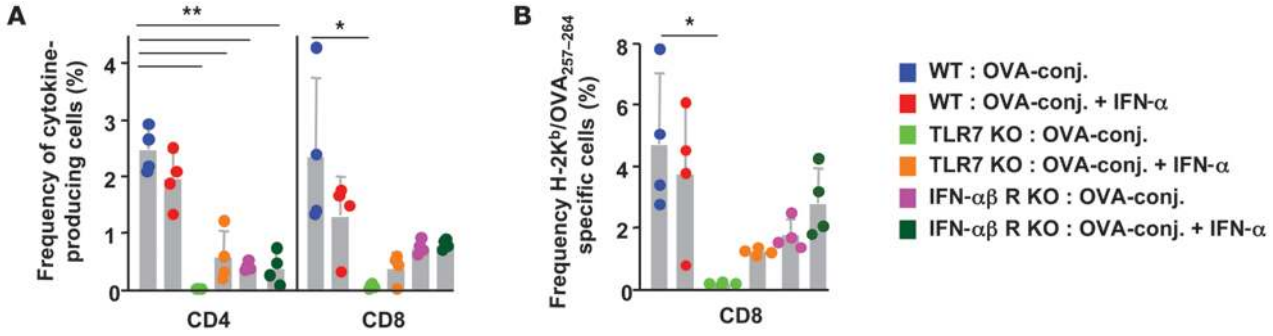

Figure 6

TLR7 and type I IFN influence T cell priming after immunization with OVA-conjugate vaccine. B6, TLR7 KO, or IFN-αβ receptor (R) KO mice (n = 4/group) were immunized as described above (see Figure 5). As indicated for some groups, IFN-α was given together with the conjugate vaccine. (**A**) Frequency of OVA-specific IFN-γ–, IL-2–, or TNF-α–producing CD4$^+$ or CD8$^+$ T cells. (**B**) Frequency of H-2K^b/OVA$_{257–264}$ tetramer–specific CD8$^+$ T cells. Each symbol represents an individual mouse. Data are representative of 2 independent experiments. *P < 0.05; **P < 0.01.

the OVA-conjugate vaccine, which was the time of the peak DC response in terms of cell numbers and antigen uptake. These cells were then sorted into CD8$^+$ DCs, pDCs, CD8$^-$DEC205$^+$ cells, and CD8$^-$DEC205$^-$ cells (Figure 7A). Graded numbers of the sorted DC subsets were added to naive OT-I or OT-II cells labeled with CFSE, and their relative potency to present or cross-present antigen was assessed based on the dilution of CFSE 3 days later. Despite the fact that pDCs took up the vaccine with higher MFI than other DC subsets and expressed TLR7, which would allow direct activation by the conjugate vaccine, they were unable to present antigen to either naive OT-I or OT-II cells in this assay (Figure 7, B and C). By contrast, CD8$^+$ DCs and surprisingly migratory CD8$^-$DEC205$^+$ DCs were comparably efficient for inducing proliferation of OT-I and OT-II cells. Finally, CD8$^-$DEC205$^-$ DCs had modest capacity to induce proliferation of OT-II cells but not OT-I cells (Figure 7, B and C). Thus, on a per cell basis, resident CD8$^+$ DCs and migratory CD8$^-$DEC205$^+$ DCs were the most potent DC populations for presenting antigen to naive OT-I and OT-II cells ex vivo using this conjugate formulation.

As noted in Figure 1, CD8$^-$DEC205$^+$ DCs are heterogeneous and can be further segregated into a relatively large population of langerin-negative dermal DCs and a far smaller number of epidermal LCs and langerin-positive dermal DCs (22, 55). Due to the potential role that such cells could have in T cell immunity, we examined the ability of these migratory DC subsets to present antigen ex vivo to naive OT-I and OT-II cells after OVA-conjugate immunization. Remarkably, as shown in Figure 7, E and F, langerin-negative dermal DCs (CD8$^-$DEC205$^+$CD103$^-$CD326$^-$) efficiently presented antigen to both OT-I and OT-II T cells, while langerin-positive dermal DCs (CD8$^-$DEC205$^+$CD103$^+$) had less capacity for T cell activation. Of note, epidermal LCs (CD8$^-$DEC205$^+$CD103$^-$CD326$^+$) showed some ability to induce OT-I but not OT-II proliferation. These data further establish that CD8$^+$ DCs and langerin-negative dermal DCs are highly efficient for antigen presentation to naive OT-I and OT-II cells ex vivo.

CD8$^-$DEC205$^+$CD103$^-$ DCs influence Th1 CD4$^+$ and CD8$^+$ T cell responses. To extend these findings, because CD8$^+$ DCs and to a lesser extent langerin-positive dermal DCs presented antigen to OT-I and OT-II cells ex vivo, we examined their role in priming T cell responses in vivo, using BATF3 KO mice, which are deficient for these DC subsets. Consistent with prior studies (60), there was a significant decrease in CD8$^+$ T cell responses in the BATF3 KO mice compared with that in WT mice (Figure 8B) using the conjugate vaccine. However, despite the potent ability of CD8$^+$ DCs to present antigen to OT-II cells ex vivo (Figure 7C), CD4$^+$ T cell responses were not affected in BATF3 KO mice after conjugate immunization (Figure 8A). These data suggest that other DC subsets are mediating Th1 CD4$^+$ T cell immunity and contribute to the residual CD8$^+$ T cell responses in these mice. To address this issue, we sorted the remaining CD11c$^+$ DC subsets (CD8$^-$DEC205$^+$CD103$^-$, CD8$^-$DEC205$^-$, and pDCs) from BATF3 KO mice after immunization with the OVA-conjugate vaccine and assessed their ability to present antigen to naive CFSE-labeled OT-I and OT-II cells ex vivo (Figure 8C). Consistent with data in Figure 7, CD8$^-$DEC205$^+$CD103$^-$ DCs isolated ex vivo from BATF3 KO mice were highly efficient for driving proliferation of naive OT-I and OT-II cells (Figure 8, D and E).

Discussion

Successful vaccines against a variety of intracellular infections will require generation of broad humoral and cellular immune responses. Analysis of the innate mechanisms that control the immunogenicity and antigenicity of the vaccine necessary for induction of such responses will be a critical step for rational vaccine design. In this report, we show that altering the formulation of a protein vaccine with a TLR agonist capable of activating multiple DC subsets can lead to improved antigen presentation and generation of multifunctional T cell responses.

Aggregation of the conjugate vaccine enhances T cell immunity. Here, we elucidate 2 mechanisms for how the formulation of the protein-TLR7/8 agonist-conjugate vaccine increases antigen presentation and adaptive immunity in vivo. First, aggregation of the protein as a consequence of conjugation with the TLR7/8 agonist by chemical treatment or UV activation leads to increased uptake of antigen by DCs and is required for T cell priming in vivo. The ability of aggregated or particulate antigens to enhance cellular immunity and specifically increase the efficiency of cross-presentation has been demonstrated with a variety of antigens and formulations (61–63). Moreover, in focusing on CD8$^+$ T cell immunity, aggregated and particulate protein improves antigen access to cytoplasmic proteasomes, resulting in more efficient cross-presentation (13, 14). Overall, the in vivo data presented here provides further rationale for using aggregated or particulate antigens to improve CD8$^+$ T cell immunity with protein-based vaccines.

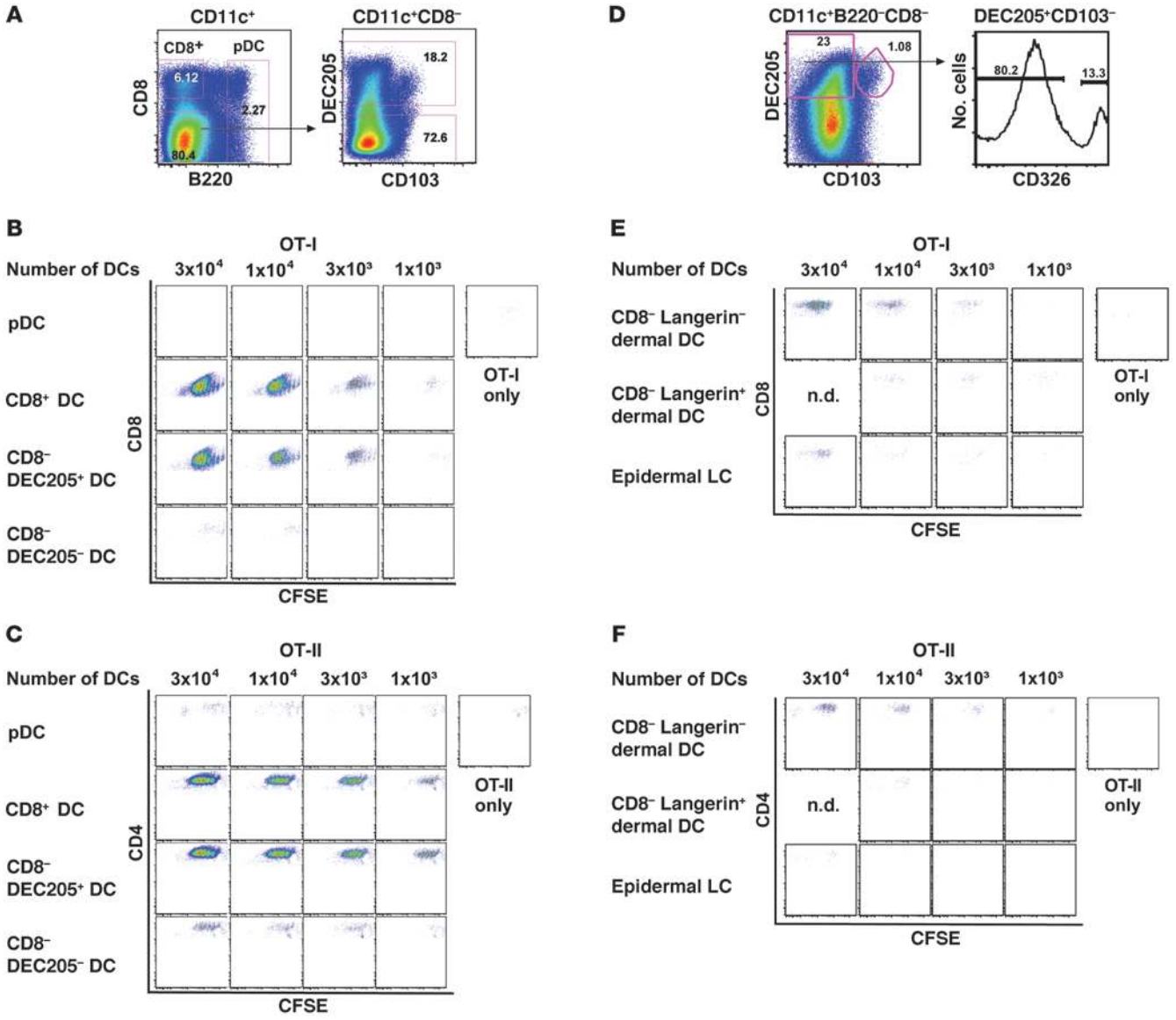

Figure 7

Resident CD8+ DCs and migratory CD205+CD103− dermal DCs provide enhanced antigen presentation to naive CD4+ and CD8+ T cells. B6 mice (n = 35–50) were immunized with 20 μg OVA-conjugate, and, 48 hours after immunization, DLNs were pooled, sorted, and cocultured with 5×10^4 CFSE-labeled OT-I or OT-II T cells. (**A** and **D**) Gating strategy for sorting of DC subsets. Numbers in gates represent the frequency of gated cells. The purity of the cell populations assessed after the sort was approximately 96%. CFSE profiles of (**B** and **E**) OT-I or (**C** and **F**) OT-II cells cocultured for 60 hours with serial dilution of sorted DC subsets. OT-I (CD8) or OT-II (CD4) cells without DCs served as negative controls. Each stimulation condition was performed in duplicate (n.d., not done). Data are representative of 3 separate experiments.

A second mechanism to explain the potency of the conjugate vaccine for T cell immunity relates to the role of TLR7/8 activation on the dynamics of DC migration and the frequency and amount of antigen taken up by DCs. TLR7/8 activation dramatically increased the number of DCs in the LN after immunization with the conjugate vaccine compared with that after immunization protein with or without free TLR7/8 agonist. Importantly, the effect of TLR7/8 activation appears to be strongly influenced by type I IFN (Figure 3C). Accordingly, both TLR7 activation and type I IFN have been shown to increase CCR7 expression on DCs and enhance the migration of DCs into lymphoid tissue (57, 58, 64–66). Indeed, the presence of type I IFN increased the uptake (~2 fold) of the conjugate vaccine by DCs from TLR7 KO mice in vivo (Figure 3C). Therefore, in addition to the direct role that type I IFN has on DC function (67–70) to enhance T cell immunity (68, 70), our data highlights how this cytokine also influences antigen presentation in the relevant lymphoid tissue site (the DLN) through enhanced migration and uptake of antigen by these DCs.

While the mechanism for the increase in uptake mediated through TLR7 and type I IFN is unclear, prior studies showed that LPS can transiently enhance uptake of soluble antigens (71) and immune complexes (72) to facilitate intracellular processing of protein for cross-presentation in vitro (14). The ability of TLR7 activation and type I IFN to influence antigen presentation in vivo

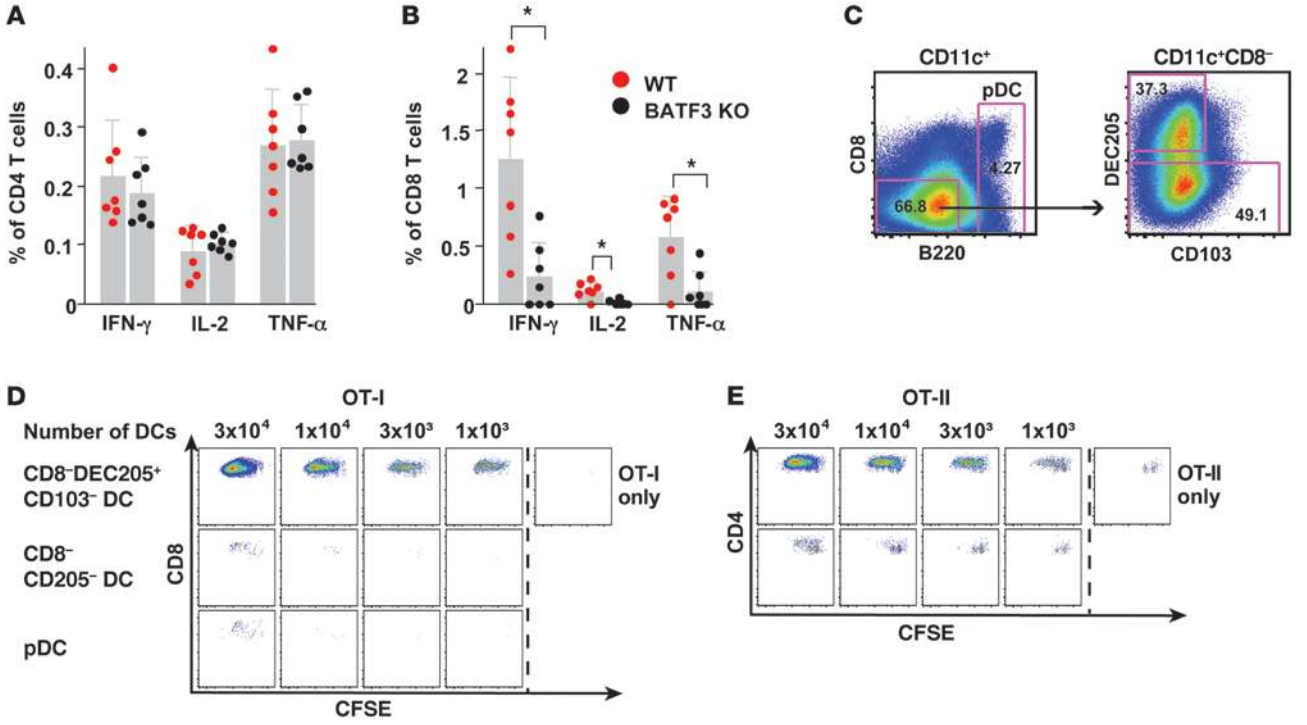

Figure 8

CD8⁻DEC205⁺CD103⁻ dermal DCs influence Th1 CD4⁺ and CD8⁺ T cell immunity. BATF3 KO mice or littermate controls (WT) were immunized with OVA-conjugate. Splenocytes were harvested 10 days after immunization, and antigen-specific cytokine production was analyzed for (**A**) CD4⁺ or (**B**) CD8⁺ T cells. Results shown represent the mean ± SD of 2 independent experiments with $n = 3–4$ mice per group. DEC205⁺CD103⁻ dermal DCs efficiently induce CD4⁺ and CD8⁺ T cell proliferation. BATF3 KO mice ($n = 17$) were immunized with the OVA-conjugate vaccine, and DLNs were harvested and pooled 48 hours after immunization. DC subsets were immediately sorted ex vivo and cocultured with 5×10^4 CFSE-labeled naive OT-I or OT-II T cells. (**C**) Gating strategy for sorting of DC subsets. Numbers in gates represent the frequency of gated cells. The purity of the cell populations assessed after the sort was more than 96%. CFSE profiles of (**D**) OT-I or (**E**) OT-II cells cocultured for 60 hours with serial dilution of sorted DC subsets. As negative controls, OT-I (CD8) or OT-II (CD4) cells alone were used. Each symbol represents an individual mouse. Each stimulation was performed in duplicate. *$P < 0.05$.

also requires conjugation of the TLR7/8 agonist to the aggregated protein, possibly by providing a more sustained innate signal in the LN or by ensuring effective activation of precisely those DCs that acquire antigen and thus are relevant for T cell activation. In this regard, prior reports showed that TLR7 or TLR9 ligands complexed with cationic lipids or carrier proteins influence the magnitude, quality, and duration of endosomal TLR signaling in DCs, leading to enhanced production of type I IFN or IL-12 (25, 73–75). Indeed we show that IL-12p40 is only produced in DCs of mice immunized with the conjugate vaccine but not with OVA protein and an excess of free TLR7/8 agonist. Thus, the presence of the aggregated conjugate vaccine in DCs and the medullary sinuses of DLNs (Supplemental Figure 2) after conjugate immunization may provide more antigen presentation (62) and durable innate signaling in the DLN, allowing for improved T cell priming.

Influence of synchronous presentation and TLR activation on T cell immunity. The codelivery of antigen and the TLR7/8 agonist to the same DC is designed to mimic the in vivo response to various pathogens (17). The ability of the conjugate vaccine to induce IL-12p40 from CD11c⁺CD8⁻ DCs, which were the largest population of DCs taking up the vaccine and shown to induce proliferation of naive OT-II cells in vitro, was distinct from the response seen with protein given with free TLR7/8 agonist. Together, these results provide strong evidence for the importance of coupled innate activation and antigen presentation by the same DC for Th1 CD4⁺ T cell immunity. These data are consistent with the seminal findings by Blander and Medzhitov (23), Sporri and Reis e Sousa (24), and others (25) that efficient class II presentation and Th1 differentiation is induced by TLR activation of DCs presenting the antigen (14). Others have also examined a requirement for coupling of antigen delivery to and TLR signaling in DCs in the generation of CD8⁺ T cell immunity through cross-presentation. Coactivation of DCs presenting protein or viral antigens with TLR3 or TLR4 ligands improved cross-presentation in vitro and in vivo (14, 76–78). By contrast, CD8⁺ T cell responses can be generated in vivo in the absence of TLR3 after immunization with protein antigens and poly (I:C) (79, 80). Here, we show that CD11c⁺CD8⁺ DCs have a critical role in cross-presentation (see below). In terms of whether such cells are directly activated by TLR7, prior analysis using quantitative PCR (42, 56), proteomics (81), or genomic profiling (82) show little to no detectable expression of TLR7 in freshly isolated CD8⁺ DCs from spleen. However, there are reports showing increased IL-12p40 production (47) and expression of costimulatory molecules from splenic CD8⁺ DCs after activation with TLR7 agonists in vivo, suggesting that TLR7 agonists may be induced in DCs upon activation in vivo or are activated indirectly. To address this we assessed mRNA from various DC subsets in LNs of WT mice for

Tlr7 expression. As shown in Supplemental Figure 7 and consistent with prior data, *Tlr7* expression was highest in pDCs compared with that in $CD8^+$ or $CD8^-DEC205^+CD103^-$ migratory dermal DCs, which include the langerin-negative dermal DCs and LCs. Taken together, these data suggest that cross-presentation by $CD11c^+CD8^+$ DCs and $CD8^-DEC205^+CD103^-$ migratory langerin-negative dermal DCs may be independent of direct TLR7/8 signaling but require bystander activation through type I IFN.

Several groups have reported that type I IFN from nonantigen-presenting DCs and nonhematopoietic stromal cells through MDA-5 can play a critical role for maximizing Th1 $CD4^+$ T cell and $CD8^+$ T responses (25, 68, 80, 83), thereby substantiating a bystander role for this cytokine (84). Indeed, we show that low but detectable Th1 $CD4^+$ and $CD8^+$ T cell responses can be elicited in the complete absence of TLR7/8 signaling after immunization with the conjugate vaccine and exogenous IFN-α. Furthermore, IFN-αβ receptor KO mice had a striking decrease in Th1 $CD4^+$ and $CD8^+$ T cell immunity in vivo after conjugate immunization, confirming a critical role of type I IFN for T cell priming in vivo. In conclusion, direct TLR stimulation of DCs presenting MHC class I and II antigen and paracrine production of type I IFN from pDCs, nonhematopoietic stromal cells, or both may be an effective approach for maximizing a Th1 $CD4^+$ and $CD8^+$ T cell response.

Engagement of multiple DC subsets is critical for Th1 $CD4^+$ and $CD8^+$ T cell immunity. The other major aim of this study was to delineate the influence that distinct DCs subsets had on the generation of Th1 $CD4^+$ T cell and $CD8^+$ T cell responses. For naive $CD4^+$ T cell activation, on a per cell basis, DLN resident and blood-derived $CD8^-DEC205^-$ DCs or migratory langerin-positive dermal DCs were far less efficient compared with langerin-negative dermal DCs or resident $CD8^+$ DCs when assessed ex vivo after conjugate immunization (Figure 7, C and F). However, Th1 $CD4^+$ T cell responses in BATF3 KO mice were comparable to those of WT mice after conjugate immunization. These data show that $CD8^+$ DCs and langerin-positive dermal DCs are dispensable for Th1 priming in vivo (60, 85) and suggest that the langerin-negative dermal DCs were mediating such priming (Figure 8). Our results contrast to a recent report by King et al. showing that langerin-positive dermal DCs were required for Th1 priming in vivo after s.c. immunization with MOG/CFA (86) and highlight how different populations of migratory dermal DC subsets can influence Th1 $CD4^+$ T cell immunity, depending on the type of innate stimulation, formulation, and site of skin immunization. Last, while langerin-expressing migratory DCs can have varying effects on DTH and CD4 immunity in other mouse models (22, 53, 87–93), we were unable to demonstrate any decrease in Th1 $CD4^+$ T cells in langerin DTR mice treated with DT or langerin DTA mice (data not shown) after immunization with the conjugate vaccine. Our results highlighting a prominent role for langerin-negative dermal DCs complement other studies showing that migratory $CD11b^+$ submucosal or dermal DCs that are langerin-negative present antigen to $CD4^+$ T cells in response to mucosal HSV infection or FITC skin painting (53, 94–96). Migratory dermal DCs can also influence $CD4^+$ Th2 immunity when protein is administered with papain (97). Thus, these data demonstrate the plasticity of dermal DCs in controlling the type $CD4^+$ T cell response, depending on the adjuvant and formulation of the protein.

For priming $CD8^+$ T cell immunity, we substantiated the efficiency by which $CD8^+$ DCs cross-present protein antigen to naive $CD8^+$ T cells (60, 78, 85, 98, 99). Remarkably, we also found that $CD8^-DEC205^+CD103^-$ migratory langerin-negative dermal DCs from WT (Figure 7E) and BATF3 KO mice (Figure 8D) are comparable to $CD8^+$ DCs in inducing proliferation of OT-I cells ex vivo. While a subset of $CD11b^-CD8^-$ (100, 101) or $CD8^-CD103^-$ DCs in the lung have been shown play a critical role for $CD8^+$ T cell immunity after influenza infection (102), we believe the data presented here are the first to show a role for such cells in mediating cross-presentation of protein antigens in skin DLNs after s.c. immunization with a protein vaccine.

pDCs were the remaining DC subset, which appears to have a critical but indirect role for both Th1 $CD4^+$ and $CD8^+$ T cell immunity. Although pDCs expressed TLR7 and took up OVA protein with increased MFI per cell compared with the other DC subsets (Figure 2B), they had little capacity to present or cross-present antigen to naive OT-I or OT-II cells, respectively, when isolated after conjugate immunization. As such cells had increased expression of CD86 compared with pDCs from naive mice or those immunized with OVA protein alone (data not shown), it suggests they were activated. This limited ability of pDCs to prime $CD4^+$ and $CD8^+$ T cells is consistent with other studies (103, 104) but contrasts with a report by Mouries et al. (105), showing that pDCs isolated from spleen can cross-present and induce primary $CD8^+$ T cells after intravenous immunization with 9 mg of OVA protein and a TLR7 agonist. The difference in our respective findings is likely due to the different routes of immunization (i.v. versus s.c.) and a 400- to 500-fold difference in the amount of OVA protein used in the other study (105). Therefore, the relative efficiency of pDCs for cross-presenting antigen with a more physiologic route and amount of antigen appears limited compared with the other DC subsets (94). Nevertheless, as pDCs in mice are the only reported source of type I IFN in response to TLR7 stimulation with imidazoquinolines (40), they would have a critical role in T cell priming due to the mechanisms described above and reported by others (18, 42, 68, 80, 84, 106, 107).

Implications for vaccine-induced T cell immunity with protein vaccines. In summary, the findings reported here advance the concept that maximizing $Th1^+$ $CD4^+$ and $CD8^+$ T cell immunity using a protein-based vaccine will require proper formulation with an adjuvant that can activate innate immunity to induce cytokines, such as IL-12 and type I IFN (7, 50), and engage multiple resident and migratory DC subsets (7, 50). As TLR7 and TLR8 are expressed on pDCs and conventional DCs, respectively, the conjugate vaccine used here may be a promising approach for use in humans. Another protein-based vaccine platform that holds great promise for generating T cell immunity is targeting protein directly to DCs based on cell surface receptors in combination with an adjuvant. A major question that arises between the DC-targeted and the nontargeted approach is whether directly activating one distinct subset of DCs is sufficient for optimizing T cell immunity or whether there is an advantage to accessing multiple subsets with a nontargeted approach as shown here. As more is learned about how distinct DC subsets can be targeted to optimize specific antibody and T cell responses, this decision will ultimately depend on the type of response required for protection. Nevertheless, our increased understanding of how protein-based vaccines work in inducing both humoral and cell-mediated immune responses offers the possibility of using optimized approaches for HIV, malaria, and tuberculosis, for which broad-based immunity will be required.

Methods

Animals. BALB/c mice, C57BL/6 (B6) mice, Pep Boy mice (CD45.1 congenic), and OT-I, OT-II, and IL-12p40 KO mice were obtained from The Jackson Laboratory and maintained in the Vaccine Research Center Animal Care Facility under pathogen-free conditions. CD11c YFP mice were obtained from Taconic and maintained in the animal facility at the NIH. TLR7 KO mice were provided by Ross Kedl (University of Colorado, Denver, Colorado, USA). IFN-αβ receptor KO mice were provided by Brian Kelsall (NIH) and then bred and maintained in the animal facility at the NIH. Langerin DTR (108) and BATF3 KO mice were provided by Björn E. Clausen and Kennneth Murphy (University of Washington, St. Louis, Missouri, USA), respectively. BATF3 KO mice on 129 background were backcrossed to B6 for 2 generations. As controls, BATF3 KO mice were compared with WT littermates. Langerin DTA mice were provided by Daniel H. Kaplan. All experiments were conducted following the guidelines of and with the approval of the Vaccine Research Center animal care and use committee.

Immunizations. Mice were immunized with a total dose of 20 μg of OVA protein with or without TLR7/8 agonist, or conjugate vaccine, or were treated with PBS. The regimens were administered s.c. in both hind footpads in a volume of 40 μl per foot. For assessment of protein uptake by DCs, 1 injection was given. For analysis of T cell responses, mice were sacrificed 7–10 days after primary or secondary immunization, which followed 3 weeks after primary immunization. In some experiments, 2 μg IFN-α (PBL Biomedical Laboratories or provided by Ross Kedl, University of Colorado, Denver, Colorado, USA) was given together with the conjugate vaccine or 1 mg of anti–IFNαR-1 (MAR1-5A3, BioLegend) was given intraperitoneally 12–16 hours before vaccination.

Conjugation. OVA-AF488 (Invitrogen) was conjugated to a TLR7/8 agonist by UV linkage as previously described (109). Further, for some experiments, OVA, OVA-AF488, or OVA-AF647 protein were conjugated to TLR7/8 using a 2-step reaction with SMCC. OVA, OVA-AF647, or OVA-AF488 (Invitrogen) was dissolved in 0.1 M sodium phosphate, 0.15 M NaCl, 1 mM EDTA, pH 7.2, and incubated with 60-fold molar excess of SMCC (Pierce) at room temperature for 1 hour. The maleimide-activated protein was purified with a PD-10 Desalting Column (GE Healthcare) equilibrated with 0.1 M sodium phosphate, 0.15 M NaCl, 5 mM EDTA, pH 7.2. The purified protein was incubated with 2 mM of active or inactive sulfhydryl TLR7/8 agonist (3M042 or 3M044, 3M Pharmaceutical) at room temperature overnight. After conjugation was completed, the conjugation reactions were purified with a PD-10 Desalting Column (GE Healthcare) equilibrated with 0.1 M sodium phosphate, 0.15 M NaCl, pH 7.2. Fractions containing conjugated protein were pooled, concentrated, and further purified by size exclusion chromatography using 0.1 M sodium phosphate, 0.15 M NaCl, pH 7.2, for column equilibration and elution.

To determine the number of 3M042 molecules attached to each protein, we analyzed the OVA-conjugate using MALDI–mass spectrometry on a MALDI Axima CFRTMPlus (Shimadzu Biotech). We calculated that there are about 20–25 TLR7/8 agonists bound to each protein. Based on that number, we can calculate that by giving 50 μg of free TLR7/8 agonist we have an excess of about 20-fold TLR7/8 agonists compared with the amount of TLR7/8 contained in the OVA-conjugate vaccine. Size-exclusion HPLC (SE-HPLC) was used to determine the masses of the aggregated OVA-conjugates. The system used for analysis consisted of a 1200 Series SE-HPLC (Agilent Technologies) and a 300 mm × 4.6 mm TSKgel Super SW300 column (Tosoh Biosciences). Molecular weight standards containing thyroglobulin (670 kDa), bovine IgG (158 kDa), chicken ovalbumin (44 kDa), equine myoglobin (17 kDa), and vitamin B12 (1.4 kDa) (all from Bio-Rad) were used to calculate the molecular weight of the aggregated OVA-conjugates. Based on those methods, we measured the molecular weight of the aggregated OVA-conjugate vaccine as approximately 580 kD.

Antibodies. The following antibodies for flow cytometry were purchased from BD Pharmingen: purified anti-CD28 (37.51), Pe-Cy7-anti-B220 (RA3-6B2), Pacific Blue–anti-CD3 (500A2), PerCP-Cy55-anti-CD3 (145-2C11), PE-anti-CD11c (HL3), FITC-anti-CD62L (MEL-14), and Alexa700-anti-CD4 (RM4-5). The following antibodies were purchased from BioLegend: APC-Cy7-anti-CD8 (53-6.7), APC-Cy55-anti-CD19 (6D5), PerCP-Cy55-anti-CD103 (2E7), Pacific Blue–anti-NK1.1 (PK136), and biotinylated-anti-CD326. APC-anti-DEC205 (NLDC-145) was purchased from Miltenyi Biotech. APC-anti-CD86 (B7-2) and APC-anti-Pan-NK (Dx5) were purchased from eBioscience. Streptavidin-QD655 was an in-house conjugation. LIVE/DEAD Fixable Orange (OrViD) and Violet Dead Cell Stain (ViViD) were purchased from Molecular Probes, and staining was performed as described by Perfetto et al. (110). Intracellular staining was performed according to the BD Cytofix/Cytoperm Kit manufacturer's instructions using APC-anti-IL-12p40 (C15.6) that was purchased from BioLegend; APC-anti-IFN-γ (XMG1.2), PE-Cy7-anti-TNFα (MP6-XT22), and PE-anti-IL-2 (MQ1-17H12) that were purchased from BD Biosciences; or Langerin AF488 (929F3.01) that was purchased from Dendritics.

DC isolation and analysis. Popliteal LNs (herein referred to as DLNs) from both hind legs were harvested, pooled, and gently disrupted using scissors and incubated with 1 mg/ml collagenase D (Roche) and 15 μg/ml DNase (Roche) for 30 minutes at 37°C. Tissues were further homogenized, washed, and enriched for $CD11c^+$ DCs by positive selection (clone N418) using a MACS cell separation following instructions of the manufacturer's protocol (Miltenyi Biotec). Cells were then stained with the viability dye LIVE/DEAD Fixable Orange or Violet Dead Cell Stain, followed by staining with different staining panels, including B220, CD3, CD11c, CD62L and CD4, CD8, CD19, CD103, NK1.1, CD326, DEC205, CD86, and Pan-NK. To stain for IL-12p40 production, 10 μg/ml Brefeldin A (Sigma-Aldrich) was added throughout the complete DC enrichment process, including the 30 minutes collagenase digestion. Cells were resuspended in 1% paraformaldehyde, acquired on a modified BD LSR II flow cytometer, and analyzed using FlowJo software (Tree Star), Pestle (M. Roederer, VRC, NIAID, NIH, USA), and SPICE (http://exon.niaid.nih.gov/spice/; provided by Mario Roederer, NIAID, NIH).

Cell sorting. Single cell suspensions were prepared from DLNs of mice 2 days after immunization with OVA-conjugate. Cells were enriched for $CD11c^+$ by magnetic beads and sorted on a FACSAria II as follows. First, dead cells were excluded using LIVE/DEAD Fixable Orange Dead Cell Stain, followed by negative exclusion of $CD19^+$, $CD3^+$, $NK1.1^+$, and B220 high/ CD11c low cells. The remaining population was gated for 4 different DC populations: $CD8^+B220^-$ DCs and pDCs based on the expression of CD8 and B220; $B220^-CD8^-$ cells were sorted for DEC205-positive versus -negative populations based on the expression of DEC205 and CD103; and $DEC205^+CD103^-$ DCs were sorted for langerin-negative dermal DCs and epidermal LCs based on their CD326 expression. Postsort analysis showed more than 96% purity for a given subset.

Analysis of polyfunctional T cell responses. Cells were harvested from spleens at various times after vaccination, and single cell suspensions from individual mice were incubated with αCD28 and OVA protein (Pierce) or the CD8 epitope of OVA, $OVA_{257–264}$ (SIINFEKL; Biosynthesis), for detection of CD4 and CD8 responses, respectively. After 2 hours, 10 μg/ml Brefeldin A was added, and cells were incubated for an additional 4 hours. Cells were stained with the viability dye LIVE/DEAD Fixable Violet Dead Cell Stain (ViViD), followed by staining for CD3, CD4, CD8, IFN-γ, IL-2, and TNF-α using the BD Cytofix/Cytoperm Kit according to the manufacturer's instructions. Cells were resuspended in 1% paraformaldehyde, acquired on a modified BD LSR II flow cytometer, and analyzed using FlowJo software (Tree Star), Pestle (M. Roederer, VRC, NIAID, NIH, USA), and SPICE (http://exon.niaid.nih.gov/spice/; provided by Mario Roederer).

Tetramer staining. A total of 3×10^6 splenocytes per sample were washed with PBS and stained with the viability dye LIVE/DEAD Fixable Orange Dead Cell Stain (OrViD). After washing, cells were stained for 15 minutes with H-2K^b/OVA$_{257–264}$ tetramer (SIINFEKL; MHC tetramer production site, Baylor College of Medicine). Anti-CD16/CD32 antibody was added for 10 minutes followed by addition of antibodies against CD3, CD8, and CD62L for an additional 20 minutes. Cells were washed with FACS buffer (PBS plus 0.5% FCS, fixed in 1% paraformaldehyde-PBS) and analyzed by flow cytometry as described above.

Ex vivo proliferation assay. Single cell suspensions from spleens from OT-I or OT-II mice were negatively selected for CD8 or CD4 T cells, respectively, using magnetic beads following the manufacturers protocol (MACS beads, Miltenyi Biotec). For ex vivo antigen-presentation assays, T cells were labeled with 1 μM CFSE (Sigma-Aldrich). 5×10^4 CFSE-labeled OT-I or OT-II cells were cultured together for 60 hours with serial dilutions of sorted DC subsets from OVA-conjugate immunized B6 mice. Proliferation was measured by flow cytometry (LSRII, BD Biosciences) as CFSE dilution by LIVE/DEAD Fixable Violet Dead Cell Stain and CD3 and CD8 for OT-I cells or by LIVE/DEAD Fixable Violet Dead Cell Stain and CD3 and CD4 for OT-II cells.

In vivo proliferation assay. OT-I T cells were purified as described above. B6 mice (CD45.1) were injected with 1×10^5 OT-I T cells isolated from OT-I mice (CD45.2). Mice were immunized with OVA-conjugate, OVA plus free TLR7/8 agonist, or OVA alone as indicated. At different times after in vivo stimulation with the various vaccines, splenocytes were harvested and stained with the viability dye LIVE/DEAD Fixable Violet Dead Cell Stain, CD3, CD8, and CD45.2.

Bacteria. Recombinant *L. monocytogenes* OVA was a gift from H. Shen (University of Pennsylvania, School of Medicine, Philadelphia, Pennsylvania, USA). The strain was maintained as a –80°C stock in brain-heart infusion/50% glycerol (BHI/50% glycerol). Before each experiment, recombinant *L. monocytogenes* OVA was streaked onto BHI agar. A single colony was inoculated into BHI, and the culture was grown overnight at 37°C with aeration.

Infectious challenge of mice and determination of bacterial load. Mice were immunized with PBS, OVA, OVA plus free TLR7/8 agonist, or OVA-conjugate as indicated. For infection with recombinant *L. monocytogenes* OVA, mice were infected with 3×10^4 to 6×10^4 CFU in 0.2 ml PBS. Overnight cultures were serially diluted in PBS to the desired dose and injected into the lateral tail vein of mice. Inocula were plated to verify dose. Three days after infection, bacterial loads were determined by plating 10-fold serial dilutions of spleen and liver homogenates in sterile PBS on BHI agar.

Confocal microscopy. Hind footpads of CD11c YFP mice (Taconic) were injected with 30 μg Alexa Fluor 647–labeled aggregated or monomeric OVA-conjugate. DLNs were harvested after 6 hours. LNs were fixed in a 0.05 M phosphate buffer containing 0.1 M L-lysine (pH 7.4), 2 mg/ml NaIO4, and 10 mg/ml paraformaldehyde for 12 hours and then washed in phosphate buffer and dehydrated in 30% sucrose in phosphate buffer. Spleens were snap frozen in Tissue-Tek (Sakura Finetek). 30-μm frozen sections were cut and stained with LYVE-1 (Novus Biologicals) and goat anti-rabbit (Invitrogen). Images were collected on a Zeiss 7/10 confocal microscope and analyzed using Imaris software.

Quantitative RT-PCR. mRNA was extracted with the RNAqueous-4-PCR Kit (Ambion) from sorted populations of cells. mRNA was added directly to one-step quantitative RT-PCR reactions that contained iScript-iTaq enzyme mix per manufacturers instructions (Bio-Rad). Probes were labeled with FAM reporter and BHQ1 quencher (Biosearch Technologies). Reactions were run in duplicate and analyzed with an ABI 7700 real-time system (PE Applied Biosystems). For each sample, a parallel reaction was run for murine β_2-microglobulin to normalize the input mRNA amount. After normalization, the relative amounts of target mRNA were calculated by the comparative ($\Delta\Delta$)Ct method (111, 112). No amplification was detected in the absence of reverse transcription. Primers and probes were designed against the sequence for murine TLR7. Primers and/or probes all crossed exon-exon boundaries; reaction conditions were optimized, and each set had identical amplification efficiency. For real-time PCR detection, the cycling conditions were as follows: 30-minute hold at 45°C for reverse transcription, 5-minute hold at 95°C for iTaq activation, and 40 cycles of 15-second denaturation at 95°C and 1 minute at 60°C for annealing and extension. The primer sequences used were as follows: B_2M forward, 5′TGACCGGCTTGTATGCTATC3′; B_2M reverse, 5′CAGTGTGAGCCAGGATATAG3′; probe, FAM-TATACTCACGCCACCCACCGGAGAA-BHQ1; TLR7 forward, 5′TCAAAGGCTCTGCGAGT3′; and TLR7 reverse, 5′AGTCAGAGATAGGCCAGGA3′; probe, FAM-CGGTTTTCTGTTGCCTTCTCTCTGTCTCAGA-BHQ1.

Statistics. The majority of the graphs were created using FlowJo software (Tree Star), Pestle (M. Roederer, VRC, NIAID, NIH, USA), and SPICE (http://exon.niaid.nih.gov/spice/; provided by Mario Roederer), and error bars were calculated with SPICE. All data are represented as mean ± SD. Statistical analyses were done using Prism software (GraphPad) or SPICE (2-tailed Student's *t* test assuming unequal variances). Some graphs were created using Prism software (GraphPad). As indicated some statistical analysis were done using Mann-Whitney test. Differences were found to be significant when *P* was less than 0.05 or 0.01, as indicated.

Acknowledgments

This work was supported by the Intramural Program of NIAID, NIH, and DFG (KA 3091/1-1 to W. Kastenmüller). B.E. Clausen is a VIDI fellow of the Netherlands Organization for Scientific Research.

Received for publication October 13, 2010, and accepted in revised form February 16, 2011.

Address correspondence to: Robert A. Seder, Cellular Immunology Section, Vaccine Research Center, NIAID, NIH, 40 Convent Drive MSC 3025, Building 40, Room 3512, Bethesda, Maryland 20892-3005, USA. Phone: 301.594.8483; Fax: 301.480.2779; E-mail: rseder@mail.nih.gov.

1. Plotkin SA. Vaccines: correlates of vaccine-induced immunity. *Clin Infect Dis*. 2008;47(3):401–409.
2. Reed SG, Bertholet S, Coler RN, Friede M. New horizons in adjuvants for vaccine development. *Trends Immunol*. 2009;30(1):23–32.
3. Gamvrellis A, Leong D, Hanley JC, Xiang SD, Mottram P, Plebanski M. Vaccines that facilitate antigen entry into dendritic cells. *Immunol Cell Biol*. 2004;82(5):506–516.
4. Obst R, van Santen HM, Mathis D, Benoist C. Antigen persistence is required throughout the expansion phase of a CD4(+) T cell response. *J Exp Med*. 2005;201(10):1555–1565.
5. Trinchieri G. Interleukin-12 and the regulation of innate resistance and adaptive immunity. *Nat Rev Immunol*. 2003;3(2):133–146.
6. Mattei F, Schiavoni G, Tough DF. Regulation of immune cell homeostasis by type I interferons. *Cytokine Growth Factor Rev*. 2010;21(4):227–236.
7. Pulendran B, Ahmed R. Translating innate immunity into immunological memory: implications for vaccine development. *Cell*. 2006;124(4):849–863.
8. Steinman RM, Banchereau J. Taking dendritic cells into medicine. *Nature*. 2007;449(7161):419–426.
9. Song R, Harding CV. Roles of proteasomes, transporter for antigen presentation (TAP), and beta 2-microglobulin in the processing of bacterial or particulate antigens via an alternate class I MHC processing pathway. *J Immunol*. 1996;156(11):4182–4190.
10. Ackerman AL, Cresswell P. Cellular mechanisms governing cross-presentation of exogenous antigens. *Nat Immunol*. 2004;5(7):678–684.
11. Houde M, et al. Phagosomes are competent organelles for antigen cross-presentation. *Nature*. 2003;425(6956):402–406.
12. Guermonprez P, Saveanu L, Kleijmeer M, Davoust J, Van Endert P, Amigorena S. ER-phagosome fusion defines an MHC class I cross-presentation compartment in dendritic cells. *Nature*. 2003;425(6956):397–402.
13. Burgdorf S, Kautz A, Bohnert V, Knolle PA, Kurts C. Distinct pathways of antigen uptake and

intracellular routing in CD4 and CD8 T cell activation. *Science*. 2007;316(5824):612–616.
14. Burgdorf S, Scholz C, Kautz A, Tampe R, Kurts C. Spatial and mechanistic separation of cross-presentation and endogenous antigen presentation. *Nat Immunol*. 2008;9(5):558–566.
15. Kovacsovics-Bankowski M, Clark K, Benacerraf B, Rock KL. Efficient major histocompatibility complex class I presentation of exogenous antigen upon phagocytosis by macrophages. *Proc Natl Acad Sci U S A*. 1993;90(11):4942–4946.
16. Akira S, Takeda K, Kaisho T. Toll-like receptors: critical proteins linking innate and acquired immunity. *Nat Immunol*. 2001;2(8):675–680.
17. Iwasaki A, Medzhitov R. Regulation of adaptive immunity by the innate immune system. *Science*. 2010;327(5963):291–295.
18. Le Bon A, et al. Direct stimulation of T cells by type I IFN enhances the CD8+ T cell response during cross-priming. *J Immunol*. 2006;176(8):4682–4689.
19. Le Bon A, et al. Cross-priming of CD8+ T cells stimulated by virus-induced type I interferon. *Nat Immunol*. 2003;4(10):1009–1015.
20. Dudziak D, et al. Differential antigen processing by dendritic cell subsets in vivo. *Science*. 2007;315(5808):107–111.
21. Shortman K, Liu YJ. Mouse and human dendritic cell subtypes. *Nat Rev Immunol*. 2002;2(3):151–161.
22. Henri S, et al. CD207+ CD103+ dermal dendritic cells cross-present keratinocyte-derived antigens irrespective of the presence of Langerhans cells. *J Exp Med*. 2010;207(1):189–206.
23. Blander JM, Medzhitov R. Toll-dependent selection of microbial antigens for presentation by dendritic cells. *Nature*. 2006;440(7085):808–812.
24. Sporri R, Reis e Sousa C. Inflammatory mediators are insufficient for full dendritic cell activation and promote expansion of CD4+ T cell populations lacking helper function. *Nat Immunol*. 2005;6(2):163–170.
25. Hou B, Reizis B, DeFranco AL. Toll-like receptors activate innate and adaptive immunity by using dendritic cell-intrinsic and -extrinsic mechanisms. *Immunity*. 2008;29(2):272–282.
26. Khan S, et al. Distinct uptake mechanisms but similar intracellular processing of two different toll-like receptor ligand-peptide conjugates in dendritic cells. *J Biol Chem*. 2007;282(29):21145–21159.
27. Huleatt JW, et al. Vaccination with recombinant fusion proteins incorporating Toll-like receptor ligands induces rapid cellular and humoral immunity. *Vaccine*. 2007;25(4):763–775.
28. Tighe H, et al. Conjugation of protein to immunostimulatory DNA results in a rapid, long-lasting and potent induction of cell-mediated and humoral immunity. *Eur J Immunol*. 2000;30(7):1939–1947.
29. Maurer T, et al. CpG-DNA aided cross-presentation of soluble antigens by dendritic cells. *Eur J Immunol*. 2002;32(8):2356–2364.
30. Cho HJ, et al. Immunostimulatory DNA-based vaccines induce cytotoxic lymphocyte activity by a T-helper cell-independent mechanism. *Nat Biotechnol*. 2000;18(5):509–514.
31. Heit A, et al. Cutting edge: Toll-like receptor 9 expression is not required for CpG DNA-aided cross-presentation of DNA-conjugated antigens but essential for cross-priming of CD8 T cells. *J Immunol*. 2003;170(6):2802–2805.
32. Hornung V, et al. Quantitative expression of toll-like receptor 1-10 mRNA in cellular subsets of human peripheral blood mononuclear cells and sensitivity to CpG oligodeoxynucleotides. *J Immunol*. 2002;168(9):4531–4537.
33. Kadowaki N, et al. Subsets of human dendritic cell precursors express different toll-like receptors and respond to different microbial antigens. *J Exp Med*. 2001;194(6):863–869.
34. Jarrossay D, Napolitani G, Colonna M, Sallusto F, Lanzavecchia A. Specialization and complementarity in microbial molecule recognition by human myeloid and plasmacytoid dendritic cells. *Eur J Immunol*. 2001;31(11):3388–3393.
35. Diebold SS, Kaisho T, Hemmi H, Akira S, Reis e Sousa C. Innate antiviral responses by means of TLR7-mediated recognition of single-stranded RNA. *Science*. 2004;303(5663):1529–1531.
36. Heil F, et al. Species-specific recognition of single-stranded RNA via toll-like receptor 7 and 8. *Science*. 2004;303(5663):1526–1529.
37. Lund JM, et al. Recognition of single-stranded RNA viruses by Toll-like receptor 7. *Proc Natl Acad Sci U S A*. 2004;101(15):5598–5603.
38. Gorden KB, et al. Synthetic TLR agonists reveal functional differences between human TLR7 and TLR8. *J Immunol*. 2005;174(3):1259–1268.
39. Heil F, et al. The Toll-like receptor 7 (TLR7)-specific stimulus loxoribine uncovers a strong relationship within the TLR7, 8 and 9 subfamily. *Eur J Immunol*. 2003;33(11):2987–2997.
40. Hemmi H, et al. Small anti-viral compounds activate immune cells via the TLR7 MyD88-dependent signaling pathway. *Nat Immunol*. 2002; 3(2):196–200.
41. Jurk M, et al. Human TLR7 or TLR8 independently confer responsiveness to the antiviral compound R-848. *Nat Immunol*. 2002;3(6):499.
42. Doxsee CL, Riter TR, Reiter MJ, Gibson SJ, Vasilakos JP, Kedl RM. The immune response modifier and Toll-like receptor 7 agonist S-27609 selectively induces IL-12 and TNF-alpha production in CD11c+CD11b+CD8- dendritic cells. *J Immunol*. 2003;171(3):1156–1163.
43. Demaria O, et al. TLR8 deficiency leads to autoimmunity in mice. *J Clin Invest*. 2010;120(10):3651–3662.
44. Ahonen CL, et al. Combined TLR and CD40 triggering induces potent CD8+ T cell expansion with variable dependence on type I IFN. *J Exp Med*. 2004;199(6):775–784.
45. Gorden KK, Qiu XX, Binsfeld CC, Vasilakos JP, Alkan SS. Cutting edge: activation of murine TLR8 by a combination of imidazoquinoline immune response modifiers and polyT oligodeoxynucleotides. *J Immunol*. 2006;177(10):6584–6587.
46. Martinez J, Huang X, Yang Y. Toll-like receptor 8-mediated activation of murine plasmacytoid dendritic cells by vaccinia viral DNA. *Proc Natl Acad Sci U S A*. 2010;107(14):6442–6447.
47. Rajagopal D, Paturel C, Morel Y, Uematsu S, Akira S, Diebold SS. Plasmacytoid dendritic cell-derived type I interferon is crucial for the adjuvant activity of Toll-like receptor 7 agonists. *Blood*. 2010;115(10):1949–1957.
48. Wille-Reece U, et al. HIV Gag protein conjugated to a Toll-like receptor 7/8 agonist improves the magnitude and quality of Th1 and CD8+ T cell responses in nonhuman primates. *Proc Natl Acad Sci U S A*. 2005;102(42):15190–15194.
49. Wille-Reece U, Wu CY, Flynn BJ, Kedl RM, Seder RA. Immunization with HIV-1 Gag protein conjugated to a TLR7/8 agonist results in the generation of HIV-1 Gag-specific Th1 and CD8+ T cell responses. *J Immunol*. 2005;174(12):7676–7683.
50. Pulendran B, Tang H, Denning TL. Division of labor, plasticity, and crosstalk between dendritic cell subsets. *Curr Opin Immunol*. 2008;20(1):61–67.
51. Randolph GJ, Ochando J, Partida-Sanchez S. Migration of dendritic cell subsets and their precursors. *Annu Rev Immunol*. 2008;26:293–316.
52. Henri S, et al. Disentangling the complexity of the skin dendritic cell network. *Immunol Cell Biol*. 2010;88(4):366–375.
53. Shklovskaya E, Roediger B, Fazekas de St Groth B. Epidermal and dermal dendritic cells display differential activation and migratory behavior while sharing the ability to stimulate CD4+ T cell proliferation in vivo. *J Immunol*. 2008;181(1):418–430.
54. Merad M, Ginhoux F, Collin M. Origin, homeostasis and function of Langerhans cells and other langerin-expressing dendritic cells. *Nat Rev Immunol*. 2008;8(12):935–947.
55. Bedoui S, et al. Cross-presentation of viral and self antigens by skin-derived CD103+ dendritic cells. *Nat Immunol*. 2009;10(5):488–495.
56. Edwards AD, et al. Toll-like receptor expression in murine DC subsets: lack of TLR7 expression by CD8 alpha+ DC correlates with unresponsiveness to imidazoquinolines. *Eur J Immunol*. 2003;33(4):827–833.
57. Gibson SJ, et al. Plasmacytoid dendritic cells produce cytokines and mature in response to the TLR7 agonists, imiquimod and resiquimod. *Cell Immunol*. 2002;218(1–2):74–86.
58. Asselin-Paturel C, et al. Mouse type I IFN-producing cells are immature APCs with plasmacytoid morphology. *Nat Immunol*. 2001;2(12):1144–1150.
59. Khader SA, et al. Interleukin 12p40 is required for dendritic cell migration and T cell priming after Mycobacterium tuberculosis infection. *J Exp Med*. 2006;203(7):1805–1815.
60. Hildner K, et al. Batf3 deficiency reveals a critical role for CD8alpha+ dendritic cells in cytotoxic T cell immunity. *Science*. 2008;322(5904):1097–1100.
61. Graham DB, et al. An ITAM-signaling pathway controls cross-presentation of particulate but not soluble antigens in dendritic cells. *J Exp Med*. 2007;204(12):2889–2897.
62. Trombetta ES, Mellman I. Cell biology of antigen processing in vitro and in vivo. *Annu Rev Immunol*. 2005;23:975–1028.
63. Schnorrer P, et al. The dominant role of CD8+ dendritic cells in cross-presentation is not dictated by antigen capture. *Proc Natl Acad Sci U S A*. 2006;103(28):10729–10734.
64. Yrlid U, Milling SW, Miller JL, Cartland S, Jenkins CD, MacPherson GG. Regulation of intestinal dendritic cell migration and activation by plasmacytoid dendritic cells, TNF-alpha and type 1 IFNs after feeding a TLR7/8 ligand. *J Immunol*. 2006;176(9):5205–5212.
65. Parlato S, et al. Expression of CCR-7, MIP-3beta, and Th-1 chemokines in type I IFN-induced monocyte-derived dendritic cells: importance for the rapid acquisition of potent migratory and functional activities. *Blood*. 2001;98(10):3022–3029.
66. Cella M, et al. Plasmacytoid monocytes migrate to inflamed lymph nodes and produce large amounts of type I interferon. *Nat Med*. 1999;5(8):919–923.
67. Blanco P, Palucka AK, Gill M, Pascual V, Banchereau J. Induction of dendritic cell differentiation by IFN-alpha in systemic lupus erythematosus. *Science*. 2001;294(5546):1540–1543.
68. Longhi MP, et al. Dendritic cells require a systemic type I interferon response to mature and induce CD4+ Th1 immunity with poly IC as adjuvant. *J Exp Med*. 2009;206(7):1589–1602.
69. Ito T, et al. Interferon-alpha and interleukin-12 are induced differentially by Toll-like receptor 7 ligands in human blood dendritic cell subsets. *J Exp Med*. 2002;195(11):1507–1512.
70. Gallucci S, Lolkema M, Matzinger P. Natural adjuvants: endogenous activators of dendritic cells. *Nat Med*. 1999;5(11):1249–1255.
71. West MA, et al. Enhanced dendritic cell antigen capture via toll-like receptor-induced actin remodeling. *Science*. 2004;305(5687):1153–1157.
72. Gil-Torregrosa BC, et al. Control of cross-presentation during dendritic cell maturation. *Eur J Immunol*. 2004;34(2):398–407.
73. Honda K, et al. Spatiotemporal regulation of MyD88-IRF-7 signalling for robust type-I interferon induction. *Nature*. 2005;434(7036):1035–1040.
74. Guiducci C, et al. PI3K is critical for the nuclear translocation of IRF-7 and type I IFN production by human plasmacytoid predendritic cells in response to TLR activation. *J Exp Med*. 2008;205(2):315–322.

75. Wu CC, et al. Immunotherapeutic activity of a conjugate of a Toll-like receptor 7 ligand. *Proc Natl Acad Sci U S A*. 2007;104(10):3990–3995.
76. Schulz O, et al. Toll-like receptor 3 promotes cross-priming to virus-infected cells. *Nature*. 2005;433(7028):887–892.
77. Davey GM, Wojtasiak M, Proietto AI, Carbone FR, Heath WR, Bedoui S. Cutting edge: priming of CD8 T cell immunity to herpes simplex virus type 1 requires cognate TLR3 expression in vivo. *J Immunol*. 2010;184(5):2243–2246.
78. Lin ML, et al. Selective suicide of cross-presenting CD8+ dendritic cells by cytochrome c injection shows functional heterogeneity within this subset. *Proc Natl Acad Sci U S A*. 2008;105(8):3029–3034.
79. Ngoi SM, Tovey MG, Vella AT. Targeting poly(I:C) to the TLR3-independent pathway boosts effector CD8 T cell differentiation through IFN-alpha/beta. *J Immunol*. 2008;181(11):7670–7680.
80. Wang Y, Cella M, Gilfillan S, Colonna M. Cutting edge: polyinosinic:polycytidylic acid boosts the generation of memory CD8 T cells through melanoma differentiation-associated protein 5 expressed in stromal cells. *J Immunol*. 2010;184(6):2751–2755.
81. Luber CA, et al. Quantitative proteomics reveals subset-specific viral recognition in dendritic cells. *Immunity*. 2010;32(2):279–289.
82. Robbins SH, et al. Novel insights into the relationships between dendritic cell subsets in human and mouse revealed by genome-wide expression profiling. *Genome Biol*. 2008;9(1):R17.
83. Trumpfheller C, et al. The microbial mimic poly IC induces durable and protective CD4+ T cell immunity together with a dendritic cell targeted vaccine. *Proc Natl Acad Sci U S A*. 2008;105(7):2574–2579.
84. Tough DF, Borrow P, Sprent J. Induction of bystander T cell proliferation by viruses and type I interferon in vivo. *Science*. 1996;272(5270):1947–1950.
85. Edelson BT, et al. Peripheral CD103+ dendritic cells form a unified subset developmentally related to CD8alpha+ conventional dendritic cells. *J Exp Med*. 2010;207(4):823–836.
86. King IL, Kroenke MA, Segal BM. GM-CSF-dependent, CD103+ dermal dendritic cells play a critical role in Th effector cell differentiation after subcutaneous immunization. *J Exp Med*. 2010;207(5):953–961.
87. Kaplan DH, Jenison MC, Saeland S, Shlomchik WD, Shlomchik MJ. Epidermal langerhans cell-deficient mice develop enhanced contact hypersensitivity. *Immunity*. 2005;23(6):611–620.
88. Bursch LS, et al. Identification of a novel population of Langerin+ dendritic cells. *J Exp Med*. 2007;204(13):3147–3156.
89. Poulin LF, Henri S, de Bovis B, Devilard E, Kissenpfennig A, Malissen B. The dermis contains langerin+ dendritic cells that develop and function independently of epidermal Langerhans cells. *J Exp Med*. 2007;204(13):3119–3131.
90. Ginhoux F, et al. Blood-derived dermal langerin+ dendritic cells survey the skin in the steady state. *J Exp Med*. 2007;204(13):3133–3146.
91. Kissenpfennig A, et al. Dynamics and function of Langerhans cells in vivo: dermal dendritic cells colonize lymph node areas distinct from slower migrating Langerhans cells. *Immunity*. 2005;22(5):643–654.
92. Wang L, Bursch LS, Kissenpfennig A, Malissen B, Jameson SC, Hogquist KA. Langerin expressing cells promote skin immune responses under defined conditions. *J Immunol*. 2008;180(7):4722–4727.
93. Nagao K, et al. Murine epidermal Langerhans cells and langerin-expressing dermal dendritic cells are unrelated and exhibit distinct functions. *Proc Natl Acad Sci U S A*. 2009;106(9):3312–3317.
94. Lee HK, et al. Differential roles of migratory and resident DCs in T cell priming after mucosal or skin HSV-1 infection. *J Exp Med*. 2009;206(2):359–370.
95. Zhao X, et al. Vaginal submucosal dendritic cells, but not Langerhans cells, induce protective Th1 responses to herpes simplex virus-2. *J Exp Med*. 2003;197(2):153–162.
96. Itano AA, et al. Distinct dendritic cell populations sequentially present antigen to CD4 T cells and stimulate different aspects of cell-mediated immunity. *Immunity*. 2003;19(1):47–57.
97. Tang H, et al. The T helper type 2 response to cysteine proteases requires dendritic cell-basophil cooperation via ROS-mediated signaling. *Nat Immunol*. 2010;11(7):608–617.
98. den Haan JM, Lehar SM, Bevan MJ. CD8(+) but not CD8(–) dendritic cells cross-prime cytotoxic T cells in vivo. *J Exp Med*. 2000;192(12):1685–1696.
99. Pooley JL, Heath WR, Shortman K. Cutting edge: intravenous soluble antigen is presented to CD4 T cells by CD8- dendritic cells, but cross-presented to CD8 T cells by CD8+ dendritic cells. *J Immunol*. 2001;166(9):5327–5330.
100. Belz GT, et al. Distinct migrating and nonmigrating dendritic cell populations are involved in MHC class I-restricted antigen presentation after lung infection with virus. *Proc Natl Acad Sci U S A*. 2004;101(23):8670–8675.
101. GeurtsvanKessel CH, et al. Clearance of influenza virus from the lung depends on migratory langerin+CD11b- but not plasmacytoid dendritic cells. *J Exp Med*. 2008;205(7):1621–1634.
102. Ballesteros-Tato A, Leon B, Lund FE, Randall TD. Temporal changes in dendritic cell subsets, cross-priming and costimulation via CD70 control CD8(+) T cell responses to influenza. *Nat Immunol*. 2010;11(3):216–224.
103. Krug A, et al. Interferon-producing cells fail to induce proliferation of naive T cells but can promote expansion and T helper 1 differentiation of antigen-experienced unpolarized T cells. *J Exp Med*. 2003;197(7):899–906.
104. Salio M, Palmowski MJ, Atzberger A, Hermans IF, Cerundolo V. CpG-matured murine plasmacytoid dendritic cells are capable of in vivo priming of functional CD8 T cell responses to endogenous but not exogenous antigens. *J Exp Med*. 2004;199(4):567–579.
105. Mouries J, Moron G, Schlecht G, Escriou N, Dadaglio G, Leclerc C. Plasmacytoid dendritic cells efficiently cross-prime naive T cells in vivo after TLR activation. *Blood*. 2008;112(9):3713–3722.
106. Martin-Fontecha A, et al. Induced recruitment of NK cells to lymph nodes provides IFN-gamma for T(H)1 priming. *Nat Immunol*. 2004;5(12):1260–1265.
107. Marrack P, Kappler J, Mitchell T. Type I interferons keep activated T cells alive. *J Exp Med*. 1999;189(3):521–530.
108. Bennett CL, et al. Inducible ablation of mouse Langerhans cells diminishes but fails to abrogate contact hypersensitivity. *J Cell Biol*. 2005;169(4):569–576.
109. Wille-Reece U, et al. Toll-like receptor agonists influence the magnitude and quality of memory T cell responses after prime-boost immunization in nonhuman primates. *J Exp Med*. 2006;203(5):1249–1258.
110. Perfetto SP, et al. Amine reactive dyes: an effective tool to discriminate live and dead cells in polychromatic flow cytometry. *J Immunol Methods*. 2006;313(1–2):199–208.
111. Johnson MR, Wang K, Smith JB, Heslin MJ, Diasio RB. Quantitation of dihydropyrimidine dehydrogenase expression by real-time reverse transcription polymerase chain reaction. *Anal Biochem*. 2000;278(2):175–184.
112. Pfaffl MW. A new mathematical model for relative quantification in real-time RT-PCR. *Nucleic Acids Res*. 2001;29(9):e45.